

PRODUCTION OF ULTRA HIGH MOLECULAR WEIGHT POLY-ETHYLENE / BUTYL
RUBBER FIBERS VIA ELECTROSPINNING

by

Yahya Çađrı Öztan

B.S., Mechanical Engineering, Istanbul Technical University, 2011

Submitted to the Institute for Graduate Studies in
Science and Engineering in partial fulfillment of
the requirements for the degree of
Master of Science

Graduate Program in Mechanical Engineering
Bođaziçi University
2015

ACKNOWLEDGEMENTS

First of all, I would like to express my gratitude and respects to my thesis supervisor, Prof. Sabri Altıntaş for his encouragements and personal support to complete this thesis. I have not only learned limitless technical knowledge from his courses and words but also improved my view of world. He is surely the key to the success of this thesis. Secondly, for his limitless supports even when he lacks enough time to give, I owe a great gratitude to Assist. Prof. Mehmet İpekođlu. He is the one who maintained my hope and courage until the very last row of this work. I also owe a very important portion of my success to Prof. Adnan Teđmen who has been very tolerative to me and my work.

I also would like to thank to all my friends from Bođaziçi for they shared their friendships with me. Apart from them, I owe a great thank to Ayça for all her cooperative efforts and humanity.

Finally, it is sure that I would have not been successful without my precious family, and my beloved. May our happiness and unity prevail forever under our boundless love. I owe them much more than thanks.

ABSTRACT

PRODUCTION OF ULTRA HIGH MOLECULAR WEIGHT POLYETHYLENE (UHMWPE) / BUTYL RUBBER FIBERS VIA ELECTROSPINNING

This research covers the electrospinning of Ultra High Molecular Weight Polyethylene (UHMWPE) mixed with Butyl Rubber polymers. The optimum process parameters to electrospin the blend of these polymers in certain ratios have been found out and the SEM images of the resultant fibers were taken to comprehend the morphology. The polymers mixed in different ratios were subjected to electrospinning under controlled parameters and the effect of these parameters on the morphology was studied. The experiments were performed in a manner that only one instance of the parameters was altered each time, to see the influence of it on characterization of the fibers. The fibers obtained were of microfibers, instead of nanofibers, due to the fact that the fiber diameter must stay lower than 100 nanometers (0.1 micrometer) and the finest resultant fibers had an average diameter of $2.20 \pm 0.50 \mu\text{m}$. Average fiber diameters have been measured by 10 arbitrary diameters and were denoted with a deviation.

ÖZET

ELECTROSPINNING YÖNTEMİ İLE ULTRA YÜKSEK MOLEKÜLER AĞIRLIKLIL POLİETİLEN (UHMWPE) / BÜTİL KAUÇUK KARIŞIMINDAN LİF ELDESİ

Bu araştırma, Ultra Yüksek Moleküler Ağırlıklı Poletilen (UHMWPE) ile Bütıl Kauçuk polimerlerinin karışımının electrospinning işlemini kapsamaktadır. Bu polimerlerin belli oranlarda karışımlarının electrospin işlemindeki optimum parametreleri çıkarılmış ve sonuçta ortaya çıkan liflerin SEM resimleri, lif morfolojisini anlamak için çekilmiştir. Farklı oranlarda karıştırılan polimerler electrospinning işlemine kontrollü parametreler altında tabii tutulmuş ve bu parametrelerin morfolojiye etkisi çalışılmıştır. Deneyler, liflerin oluşumundaki etkilerinin görülmesi için her seferde sadece bir parametre değiştirilecek şekilde gerçekleştirilmiştir. Elde edilen lifler, en incesinin çapı 100 nm (0.1 mikrometre) değerinden fazla olması sebebiyle nanolif değil, mikrolif olmuştur. En ince çaplı fiberlerin ortalama çapı, $2.20 \pm 0.50 \mu\text{m}$ olarak ölçülmüştür. Ortalama çap ölçümü, 10 farklı fiber çapından ölçüm alınıp ortalama ve sapma olarak belirtilmiştir.

TABLE OF CONTENTS

ACKNOWLEDGEMENTS	iv
ABSTRACT	v
ÖZET	vi
LIST OF FIGURES	x
LIST OF TABLES	xiii
LIST OF SYMBOLS	xiv
LIST OF ACRONYMS/ABBREVIATIONS	xv
1. INTRODUCTION	1
1.1. Structure and Types of Polymers	2
1.2. Nanofibers and Production Methods	4
1.2.1. Drawing	4
1.2.2. Template Synthesis	5
1.2.3. Self-Assembly	6
1.2.4. Phase Separation	6
1.2.5. Electrospinning	6
1.3. Usage Fields of Electrospun Nanofibers	6
1.3.1. Osmosis Filtration	7
1.3.2. Bioengineering	7
1.3.3. Defense and Security Industry	7
1.3.4. Other Potential Fields of Use	7
2. LITERATURE REVIEW	9
3. EXPERIMENTAL	13
3.1. Experimental Setup	13
3.1.1. AC/DC High Voltage Supplier	13
3.1.2. Nozzle	13
3.1.3. Collector Surface	13
3.2. Performance of the Process	14
3.3. Parameters of Electrospinning	17

3.3.1. Polymer Solution Related Parameters	17
3.3.1.1. Conductivity of the Solution	17
3.3.1.2. Surface Tension	19
3.3.1.3. Dielectric Effect	19
3.3.1.4. Viscosity, Concentration and Chain Entanglement	20
3.3.1.5. Volatility of the Solvent	22
3.3.2. Process Parameters	23
3.3.2.1. Applied Voltage	23
3.3.2.2. Feed Rate	24
3.3.2.3. Distance between the Nozzle and the Collector	25
3.3.2.4. Type of the Collector	25
3.3.2.5. Nozzle Diameter	25
3.3.3. Ambience Related Parameters	26
3.3.3.1. Ambient Temperature	26
3.3.3.1. Moisture	27
3.3.3.1. Ambient Pressure	27
3.3.3.1. Ambient Gas and Air Circulation	27
3.4. Materials Used in the Process	28
3.4.1. UHMWPE	28
3.4.2. Butyl Rubber	30
3.4.3. Tetrahydrofuran	32
3.5. Experimental Procedure	32
3.5.1. Preparations of the Solutions	32
3.5.2. Preliminary Electrospinning Experiments	35
3.5.3. Results of the Preliminary Electrospinning Experiments	37
3.5.4. Experimental Setup	41
3.5.5. Investigated Parameters	43
4. RESULTS AND DISCUSSIONS	44
4.1. Applied Voltage	44
4.2. Distance between Nozzle and Collector	48
4.3. Feed Rate	52

5. CONCLUSIONS57
REFERENCES61

LIST OF FIGURES

Figure 1.1.	Homopolymer and copolymer [2]	2
Figure 1.2.	Linear and branched polymers [2]	3
Figure 1.3.	Drawing Operation [5]	5
Figure 1.4.	Usage fields of electrospun polymer nanofibers	8
Figure 2.1.	Beaded nanofibers formed during the electrospinning process [19]	10
Figure 2.2.	Whipping in a polymer being electrospun [11]	11
Figure 3.1.	Illustration of an electrospinning device [32]	14
Figure 3.2.	Taylor cone formed during electrospinning [68]	15
Figure 3.3.	Change of bead formation with respect to viscosity [23]	21
Figure 3.4.	Structure of a UHMWPE mer	29
Figure 3.5.	Chemical structure of a Butyl Rubber mer	31
Figure 3.6.	Chemical structure of Tetrahydrofuran	32
Figure 3.7.	SEM image of 12 wt% UHMWPE	37
Figure 3.8.	SEM image of 15 wt% UHMWPE	38

Figure 3.9.	SEM image of 20 wt% UHMWPE	38
Figure 3.10.	Illustration of the test equipment used in the experiments	42
Figure 3.11.	Illustration of the test equipment used in the experiments	42
Figure 4.1.	SEM image of 25/20 wt% (BR/UHMWPE) electrospun under 10 kV	44
Figure 4.2.	SEM image of 22/20 wt% (BR/UHMWPE) electrospun under 10 kV	45
Figure 4.3.	SEM image of 25/20 wt% (BR/UHMWPE) electrospun under 15 kV	46
Figure 4.4.	SEM image of 22/20 wt% (BR/UHMWPE) electrospun under 15 kV	46
Figure 4.5.	SEM image of 25/20 wt% (BR/UHMWPE) electrospun under 20 kV	47
Figure 4.6.	SEM image of 22/20 wt% (BR/UHMWPE) electrospun under 20 kV	48
Figure 4.7.	SEM image of 18/20 wt% (BR/UHMWPE) electrospun at 80 mm	49
Figure 4.8.	SEM image of 18/20 wt% (BR/UHMWPE) electrospun at 100 mm	49
Figure 4.9.	SEM image of 18/20 wt% (BR/UHMWPE) electrospun at 150 mm	50
Figure 4.10.	SEM image of 15/20 wt% (BR/UHMWPE) electrospun at 80 mm	50
Figure 4.11.	SEM image of 15/20 wt% (BR/UHMWPE) electrospun at 100 mm	51
Figure 4.12.	SEM image of 15/20 wt% (BR/UHMWPE) electrospun at 150 mm	51
Figure 4.13.	SEM image of 18/20 wt% (BR/UHMWPE) electrospun with $0.83 \text{ mm}^3/\text{s}$	53

Figure 4.14.	SEM image of 18/20 wt% (BR/UHMWPE) electrospun with 1.30 mm ³ /s53
Figure 4.15.	SEM image of 18/20 wt% (BR/UHMWPE) electrospun with 1.65 mm ³ /s54
Figure 4.16.	SEM image of 15/20 wt% (BR/UHMWPE) electrospun with 0.83 mm ³ /s54
Figure 4.17.	SEM image of 15/20 wt% (BR/UHMWPE) electrospun with 1.30 mm ³ /s55
Figure 4.18.	SEM image of 15/20 wt% (BR/UHMWPE) electrospun with 1.65 mm ³ /s55
Figure 5.1.	Change of nominal fiber diameter with applied voltage58
Figure 5.2.	Change of nominal fiber diameter with distance58
Figure 5.3.	Change of nominal bead diameter with distance59
Figure 5.4.	Change of nominal fiber diameter with feed rate60

LIST OF FIGURES

Table 3.1.	Changing of pore diameters with respect to the moisture rate [57]	27
Table 3.2.	Chemical and Mechanical Properties of UHMWPE [70]	29
Table 3.3.	Chemical and Mechanical Properties of Tetrahydrofuran [THF] [81]	32
Table 3.4.	Summary of the parameters altered in each experiment	43
Table 4.1.	Correlation of Concentration and Fiber Diameter, electrospun under 10 kV ...	45
Table 4.2.	Correlation of Concentration and Fiber Diameter, electrospun under 15 kV ...	47
Table 4.3.	Correlation of Concentration and Fiber Diameter, electrospun under 20 kV ...	48
Table 4.4.	Correlation of Concentration, Distance, Fiber and Bead Diameters, electrospun under 15 kV and 1.3 mm ³ /s	52
Table 4.5.	Correlation of Concentration, Distance, Fiber and Bead Diameters, electrospun under 15 kV and 100 mm	56

LIST OF SYMBOLS

d	Nominal Fiber Diameter
E	Elasticity Modulus
μ	Dynamic Viscosity
σ_t	Tensile Strength

LIST OF ACRONYMS/ABBREVIATIONS

AC	Alternative Current
ASTM	American Society for Testing of Materials
BR	Butyl Rubber
BSE	Back Scattered Electron
C ₂ H ₅ OH	Ethanol
CFC	Chlorofluorocarbon
DC	Direct Current
EDX	Energy Dispersive X-ray
Fr – 12	Freon – 12
LCD	Liquid – Crystal Display
LiCl	Lithium Chloride
MgCl ₂	Magnesium Chloride
M _w	Molecular Weight
NaCl	Sodium Chloride
N-DMF	Normal – Dimethylformamide
PA	Polyamide
PAA	Polyacrylic acid
PAH	Polyallylamine hydrochloride
PEO	Polyethylene Oxide
Ph	Power of Hydrogen
PIB	Polyisobutylene
PO	Polyethylene Oxide
PS	Polystyrene
PVA	Polyvinylalanine
PVP	Polyvinylpyrrolidone
SE	Secondary Electron
SEM	Scanning Electron Microscope

SF ₆	Sulphur Hexaphloride
THF	Tetrahydrofuran
UHMWPE	Ultra High Molecular Weight Polyethylene
VPSE	Variable Pressure Secondary Electron
wt%	Weight Ratio

1. INTRODUCTION

Nanotechnology utilizes materials that inhere dimensions on the scale of $1/10^9$ meter, which is approximately 10,000 times tinier than one single average human hair. Making nano-based materials take scientists much closer to controlling materials on the atomic scale, which requires much more focusing than it does in molecular scale. A common unit used in electrospinning, 1 Angstrom (A), is a frequent term used to clarify atomic scale dimensions and is equivalent to 1 nm.

The thought of controlling materials on the non-eye visible level, especially on the nano-level has become more than an interest in the past decades. Such materials have a useful potential in various applications, like bio-sciences, engineering, and even avionic applications. Even such numerous fields of interests have developed; nanotechnology still has many questions to understand.

Nanofibers have many distinct methods used to produce (all shall be explained in the future pages), yet, electrospinning is the the most popular amongst others. It is based on producing nanofibers by applying an excessively high electric field between two base points.

Electrospinning was initially patented by Formhals in a series of patents taken between 1934 and 1944. This allowed him to introduce a very consistent method to produce nanofibers [1], since it allows working on the nano scale.

Since electrospinning is a topic that still awaits many discoveries in, researches on it have raised remarkably recently, since nanotechnology is gaining importance day by day. A prominent amount of studies performed on electrospinning was on the production of polymer based nanofibers under controlled parameters.

Another important specialty of electrospinning operation is that it can be taught in a university course even in application laboratories. This aspect can make a great advantage because it contains many interdisciplinary topics like chemistry, physics, electronics etc. for it involves polymer-mixed solutions and chemical bondings. All these aspects and challenges give learners an opportunity to apply their theoretical and practical engineering formations during calculations. As a synopsis, it can be clearly stated that, teaching or studying electrospinning is a perfect way to improve the knowledge on numerous fields.

1.1. Structure and Types of Polymers

A polymer is a molecular structure consisting of a high number of (poly-) pieces (-mer) connected with a strong bond, the covalent bond. The single parts that form the total polymer are called monomers and can be either same or various. This similarity or diversity names the polymer structure either as a homopolymer (uniform monomers) or copolymer (various monomers), as shown in Figure 1.1 [2].

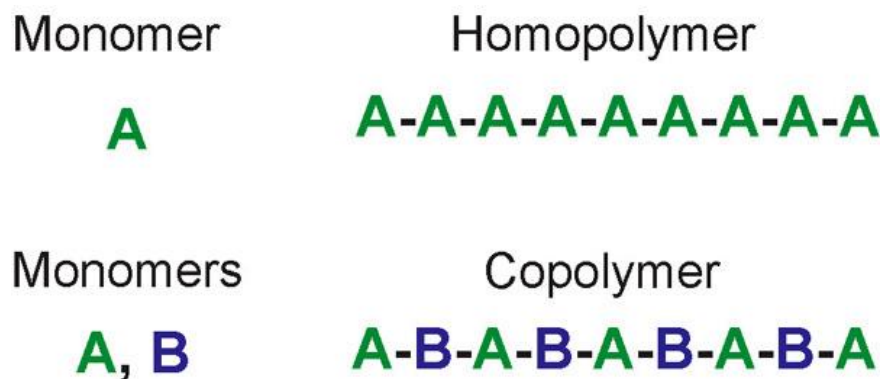


Figure 1.1. Homopolymer and copolymer [2].

The geometry of the polymeric bonds can also vary, and result with the diversity in the chemical and mechanical properties of it such as solubility, boiling and melting point, chemical inertia.

Apart from the mers, an important aspect for polymers is the structure of them, which can be linear or branched type, as shown in Figure 1.2.

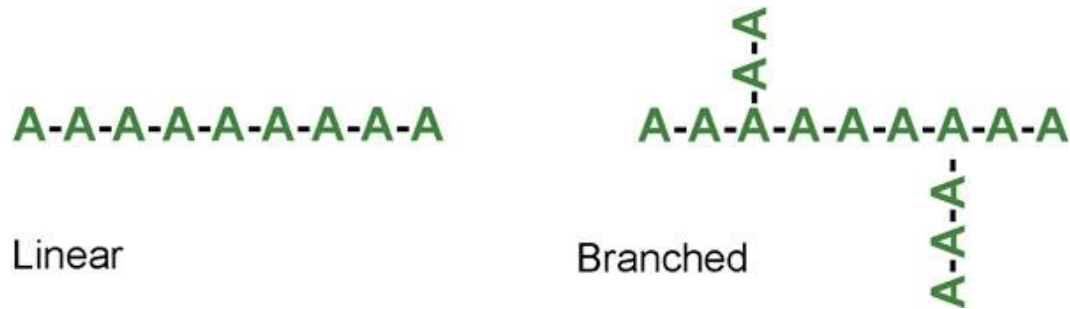


Figure 1.2. Linear and branched polymers [2].

The obtained molecules can be longer, straighter-chained, or even branched with smaller chains protruding from the endpoint of the molecule. These branches can also expand till they are connected with other branches to make a three-dimensional matrix. Molecular morphology can be counted as the most important parameter in identifying the characteristics of the polymer [3].

The size is also important and is commonly defined by molecular weight. A polymer material has monotonic repeating mers, but if it contains various chain lengths, nominal molecular weight should be taken into account. Usually, the more the molecular weight, the more the strength, yet, if polymer chains go bulkier, they become less workable and more viscous [3].

Synthetic polymers are superior to natural ones and come with more options as they can be given shape and weight in the favoured way for the propose of usage. Many of synthetic polymers inhere the potency to dissolve or melt, which allows them to be shaped in long and fine filaments and used in textile industry.

Fibers made from synthetic polymers built in organized structures which permits packing and squeezing which bring better mechanical properties to the filaments. Therefore,

filaments can be produced from variable synthetic polymers that provide lightness and the ultimate strength a polymer material can have, even more than steel [3].

Polymers have always been widely used materials since 18th century. Their unique -yet cheap- properties keep them irreplaceable with various usage fields in engineering. Besides, other fields where non-polymeric materials are utilized still experience clashes between polymers.

1.2. Nanofibers and Production Methods

Nanofibers are reckoned as fibers inhering a diameter of about one micron, or less than it. It is professionally described as structures possessing a size less than 10 nanometers. Nanofibers were named after the dimension scale, nanometer, which is equal to 10^{-9} of a meter. It is approximately as large as three atoms in row [4].

Why nanofibers have attracted this much attention lately is because they can be utilized in a very wide range like fluid filtration, biomedical applications (drug delivery, tissue scaffold), composite reinforcements and even energy supplement. Splendid mechanical and electrical characteristics of nanofibers ensure their compliance with aerospace, maritime and even electronic circuit applications, like over-capable rheostats [2,3].

So far, synthetic fibers of polymers have been produced by some processes, such as drawing, template synthesis, self-assembly, phase separation and finally, electrospinning.

1.2.1. Drawing

Drawing operation is based on the fibers that are produced by means of establishing a contiguity with a pre-solidified polymer solution using a pointed nozzle and tracking it as a viscous fiber. The composition is left to solidification by dehydration ensured by the large quantities of surface/volume ratio.

The resultant fiber can be linked with another one to form a continuous fiber structure. The process is cheap and easy, can be quickly performed. Nonetheless, allowing the drying of the solution in such an uncontrolled environment prohibits any promotes or upgrades of the process abstaining production of fine 3D fibers. Besides, the solid polymer gradually rises as time elapses because of the solvent disposition. On the other hand, rapidly increasing viscosity of the solution triggers a devastating narrowing that is the main reason of coarse fibers, which are not favorable in polymer fiber processes [5]. Figure 1.3 illustrates the operation.

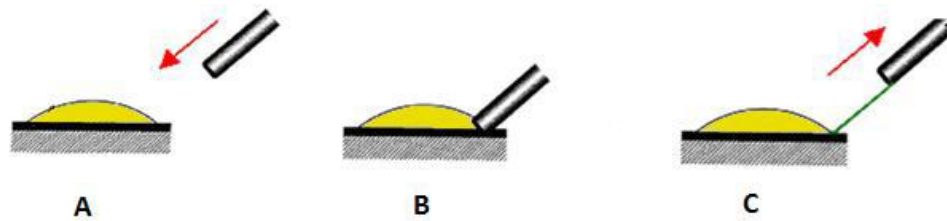


Figure 1.3. Drawing operation [5].

1.2.2. Template Synthesis

Template synthesis (or molten intercalation) is a polymer fiber production method in which inorganic product is manufactured under a polymer media. This method allows the production of hydroxide with dual coats. The resultant structures were nanocomposites. The polymer component ensures the grain growth and is blockaded beneath the coates, thus forming the polymer composite [6].

This method is not quite common although it gives the opportunity to produce treaded nanofibers. Main cons of the process are, it is held under high temperatures and the high trend of the extracellular matrix to consolidate, thus forming an undesired superstructure [6].

During the extracellular addition of the polymer, away from the solution the solved (and natural) silicate gains solubility in the same solution as the one in which the polymer is soluble,

too. This causes the polymer to adhere to the surface in mixed form. Once the solvent is discarded, the layers holding the silica-polymer composition reunite forming fibers. This method is mainly utilized on the production of polymers that are well-soluble in water. Recently, the method was started to be used in polymers that are not highly-soluble in water [6].

1.2.3. Self-Assembly

Another common method used in production of polymer fibers is self-assembly, which is based on the intercontact of the initially dispersed structures resulting with the formation of a pattern, or singularities, in the polymer matrix in the absence of an external intervention. If the base structures are molecules, then the process is named inter-molecular assembly [7].

1.2.4. Phase Separation

Phase separation is the process in which simply the polymer and the solvent can be separated by means of energy-comprising methods like cooling, heating. Gibbs phase rule is utilized in calculation of the manner through which the separation is triggered [8].

1.2.5. Electrospinning

Electrospinning is the method of aligning polymer fibers in a polymer solution applied through an electric field in the nano-scale. The equipment used in the process is pretty simple to install and start. The main components of the setup are; an area with an electric field passing through, created with a high voltage source, a tank containing a solution of a polymer and an appropriate solvent, and a nozzle from which the solvent is ejaculated in a controlled manner.

1.2. Usage Fields of Electrospun Nanofibers

Usage fields of electrospun nanofibers are wide and diverse. In the bio-medical area, they are applicable in tissue engineering, drug delivery and wound covering [10-14]. In tissue

engineering, which is another field, electrospun polymers can imitate the properties of the intercellular media in the body. They also allow users to perform researches on cell consolidation, differentiation on the small scale [10]. In wound dressing applications, polymer nanofibers prevent unwanted contaminations due to their high surface-to-volume ratio and pores small enough to avoid osmosis [10].

Recently, electrospun nanofibers have lured manufacturers quite a lot for they have splendid properties and applicability in a wide range. Usage fields can be expressed as:

1.3.1. Osmosis Filtration

Due to the alignment and regular structure of the nanofibers, they remarkably increase the filtering efficiency providing a low negative air resistance that prevents osmosis.

1.3.2. Bioengineering

Electrospun nanofibers are highly biocompatible, which means they can be permitted by the tissue matrix, and they can be used as covers that surround the pill, drug etc. to set the dissolution of them in a desired rate. They can also be utilized in scaffolds, tissue imitating structures, tumor curing and wound dressing.

1.3.3. Defence and Security Industry

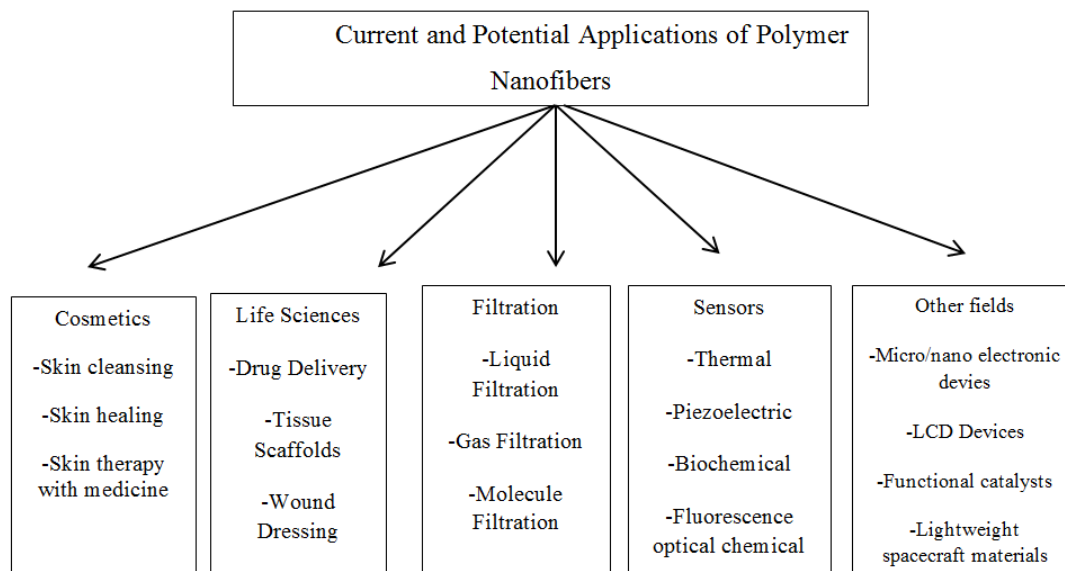
Electrospun nanofibers make a suitable material for both strong and light fighting equipment and operative military uniforms. They let air ventilation through the matrix and can prohibit penetration of harmful chemical gas threats.

1.3.4. Other Potential Fields of Use

Conductive electrospun polymers can be utilized in decharging, dissipation and even

photoelectrical devices. Besides, they can be used in textile industry, sensors and composite reinforce medium [2, 13, 29 and 61]. A chart explaining the usage fields of polymer nanofibers is given in Figure 1.4.

Figure 1.4. Usage fields of electrospun polymer nanofibers.



Other applications that electrospinning is useful for, are the manufacturing of reinforced matrix-fibers for composites, and non-soakable surfaced materials in textile engineering branch [15].

2. LITERATURE REVIEW

Since the first patent taken by Formhals [1] in 1934, roughly 60 patents were also submitted and recorded in various sub-topics and methods of electrospinning. Just before the recent revival of research performed on electrospinning, due to the rise in nanotechnology, most of the earlier researches which are now reconciled with electrospinning were done in other areas of research. Sir Geoffrey Ingram Taylor discovered that, when a polymer solution is subjected to an electric field, where it will be exposed to high electrical forces, the droplets form a conical shape and later becomes an electrically ejected jet [16]. This jet which is taken as a geometrical characteristic in electrospinning of a constant polymer solution is referred as Taylor Cone and is used in numerous experiments as a display of the ongoing process. As researches concentrated more on producing nanomaterials, electrospinning gained more importance due to its consistence in nano dial.

As scientists began to utilize electrospinning method to produce nanoscale fibers, they marked the presence of bead-like structures along the fibers once they are removed from the collector, where they are ejected upon. This fact is attributed to a capillary flow mechanism as the solution is forced through the nozzle [17, 18].

So far, the reasons of this phenomenon were not intensively investigated, and are supposed to occur since the system tends to reduce its free surface energy by forming these beads. This mechanism heavily relies on the distance between the nozzle and the collector because, if it is insufficient for these beads to distinguish from each other, beads start forming. These beads are mainly unwanted due to their deterioration of the singular geometry of the fiber. Besides, the beads are where viscous forces accumulate and form notch like imperfections through the fiber. Overcoming the bead issue requires optimization in electrospinning for bead formation is the congestion between viscous forces and the electrical forces. In order to attain this goal, the solution must be picked carefully. Such a nanofiber image taken under SEM media can be seen in Figure 2.1.

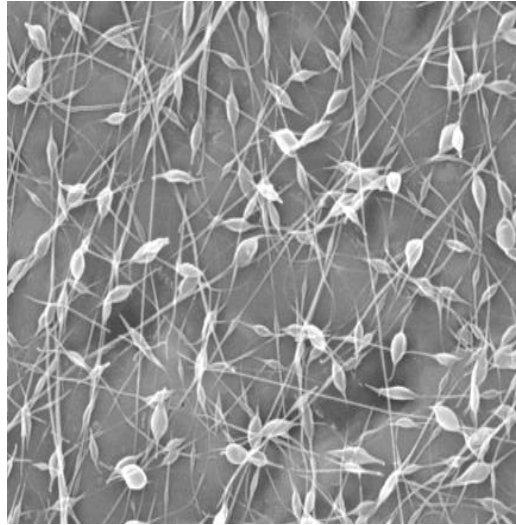


Figure 2.1. Beaded nanofibers formed during the electrospinning process [19].

Fong *et al.* stated that these beads are a consequence of excessive surface tension in the solution [18]. Excessive amount of surface tension intensifies the capillary effect aforementioned. In his research, it was proven that, reducing the surface tension will conclude with fewer beads in the fibers and increasing the radius of the fibers likewise.

Tripatanasuwan *et al.* ascribes the formation of these bead structures to the same capillary effect, yet, added that the moisture in the ambient where the process takes place may trigger a raise in the evaporation of the solution thus leading the formation of beads [17]. In the same ambience, if moisture is increased, the density of the beads was observed to increase, too. The same study also indicated that, surface tension is not the unique parameter in the formation of beads.

Tripatanasuwan *et al.* also showed the effect of moisture on the formation of the beads if other parameters like voltage, ejaculation rate, distance between the nozzle and the collector, and viscosity are held under control.

Nevertheless, by raising the space between the collector and the nozzle, altering the speed of the jet and keeping the mass rate of the flow, all can highly influence the

evaporation of the solvent liquid in the polymer solution during electrospinning.

Another important discovery on electrospinning is the fact named whipping. As the solution is forced onto the collector, the liquid component evaporates thus leaving the sole polymer behind. During this evaporation process, the jet experiences a spiring. Up to now, many researches were performed to understand why whipping occurs and model it to predict the parameters causing [20, 21].

In Yarin *et al.* tried to foresee the quantity of whipping due to the distortion effects of the electric field and the air in the ambience. This research stated that, the whipping geometry is heavily based on the evaporation of the liquid solvent and the solidification of the polymer on the collector screen.

A figurative study was made by Hohmann *et al.* and new parameters like Rayleigh instability, electrical disturbances, on occurring of whipping were introduced [23]. Figure 2.2 displays the whipping phenomenon during a spinning operation

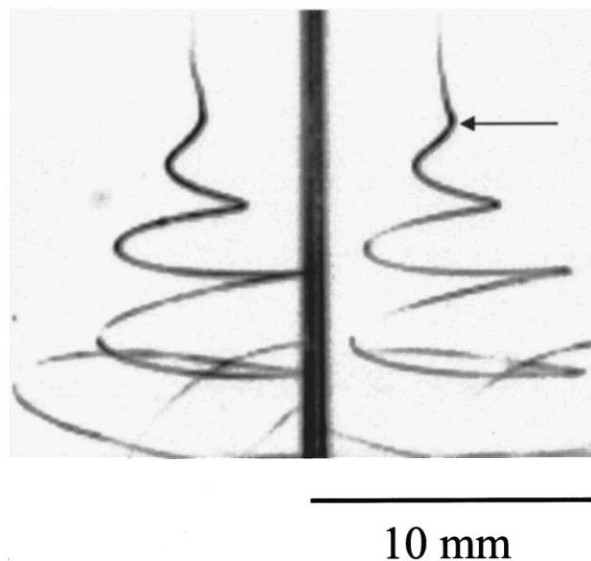


Figure 2.2. Whipping in a polymer being electrospun [11].

After bead formation and whipping phenomena were discovered, studies on electrospinning proceeded with utilization of different polymers solved in different solvents. In 2003, Huang published an article containing the list of more than 45 polymers with miscible solvents that had been electrospun including the testing variables and implementations of the products up to then [24].

Scardino *et al.* have made a research on electrospinning in 2000 and acquired a patent containing a newly introduced process type that allows producing hybrid/composite thread. The fibers produced had radii changing from 0.2 to 1 nanometer were exposed to air suction operation and afterwards joint with a carrier fiber to form linearly assembled threads [26].

Another prominent contribution to electrospinning literature was made by Baumgarten in 1971. He researched the correlations between fiber geometries, polymer solution viscosity, capillary effects, mass flow rate and Taylor cone degree. He worked on the electrospin processing of acrylo-nano based fibers. The research stated to produce nanofibers with less than 1 micron in radius [27].

A cooperative research by Larrondo and Manley in 1981 applied the parameters that were calculated their unique effect on the process, on polyethylene and polypropylene based solutions. Later, the specimens produced were exposed to a mechanical test [28, 29]

In 1995, Doshi and Reneker studied the impacts of various parameters on the fiber geometry of PO (Polyethylene Oxide) based solution [30].

3. EXPERIMENTAL

3.1. Experimental Setup

Illustration of a common electrospinning device is given in Figure 6. This basic setup consists of three parts.

3.1.1. AC/DC High Voltage Supplier

Generates high rates of electrical potentials needed to spin the fibers. Carries two distinct electrodes of one is positive and one is negative loaded. The positive electrode is attached to the nozzle and the negative one is attached to the collector surface. This enables electric forces to be applied upon the jet.

3.1.2. Nozzle

Consists of a capillary tube from which the solution is ejaculated with a desired speed, onto the collector surface. The speed –and thus, the rate- can be adjusted simply from the pump supplying the solution to the nozzle. The nozzle can be oriented either vertically or horizontally, depending on the structure of the fibers desired [31]. Also, additional nozzles are possible to utilize. This allows obtaining composite fibers, which is a distinct topic.

3.1.3. Collector Surface

The surface where electrospinning ends. On the collector is a cover that facilitates removal of the electrospun polymer from the surface. The cover is commonly an aluminum foil, which is used in the experiments of this thesis, too. The collector can also be variable. It can be deployed either horizontal, or vertical. Horizontal deployment results with randomly distributed fibers whereas vertical deployment allows directional-oriented, aligned and fine fibers, which exhibits much more different properties than the previous one. Dynamic

collectors are also applicable in this process, like rotating drums, cylinders and discs. Figure 3.1 illustrates an electrospinning device.

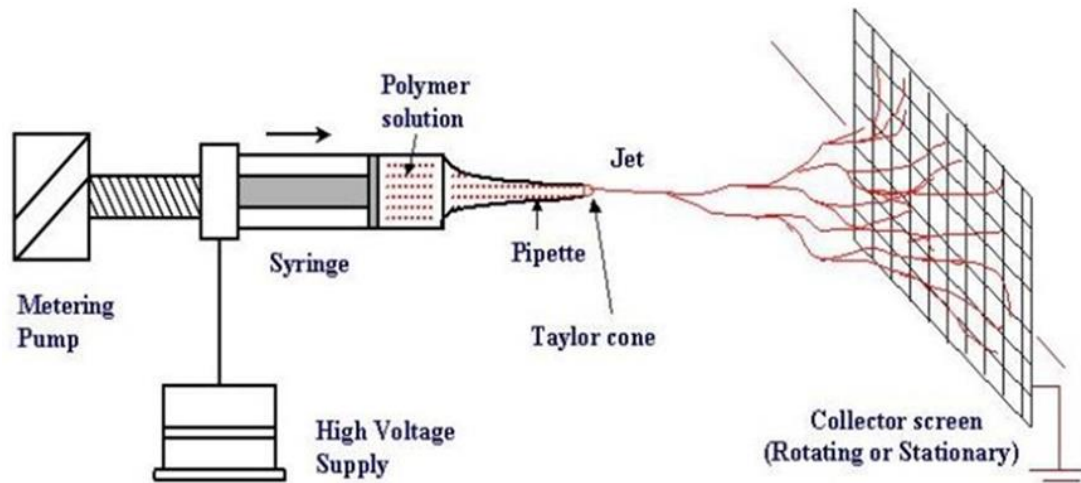


Figure 3.1. Illustration of an electrospinning device [32].

3.2. Performance of the Process

The process occurs in four phases. In the first phase, the polymer solution emerges the nozzle with a pre-set speed. Secondly, the aforementioned phenomenon, whipping occurs. In the third phase, splaying occurs on the solution due to the charging in the polymer. Finally, in the fourth phase, the sole polymer, where solvent has evaporated from, adheres to the collector [26].

If an electrostatical force is implemented via a high voltage source, upon the system, an electrical field occurs at the edge of the nozzle on which the polymer solution is kept by means of surface tension. The collection of charges in the edge triggers a repelling which is in the opposite direction of the surface tension. The more the voltage is, the more the force that repels the polymer outwards. This repelling brings a repulsion ending with formation of a conical structure at the tip of the polymer drop. This phenomenon is called Taylor cone and is illustrated in Figure 3.2 [20].

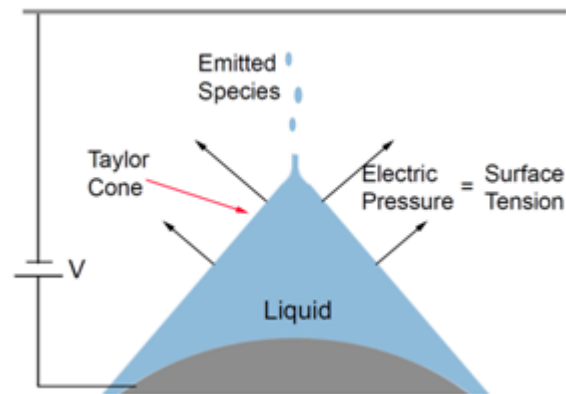


Figure 3.2. Taylor cone formed during electrospinning [68].

Taylor pointed that, a conductive liquid drop exposed to an electric field remains in statical equilibrium with an angle of about 49.3 degrees. Many recent researches state that Taylor Cone is valid under specified circumstances. Another cone angle of 33.4 degrees have been measured and calculated via both applied and theoretical methods, under threshold electric field [29]. When the repulsion force overcomes the surface tension, the drop of the solution leaves the nozzle, just at the value of Taylor Angle which forms the Taylor Cone.

The jet undergoes a short stabilization interval, but then, obtains a complex, spire-like displacement (whipping) and finally starts the unstable portion of the movement. During this unstable portion of the movement, the liquid co-forming the solution evaporates, leaving the polymer fibers behind. The process ends with the collection of the fibers on the collector surface on which the negative alligator clip is attached.

As stated before, the polymer jet forms right after it overcomes the adherent stress, the surface tension. In fact, a smooth jet form is formed on the sub-surface on the Taylor Cone.

The stable liquid jet keeps this stability till a distance [34]. This straight route is tracked by an area which is alike a liquid flowing from a laminar to a turbulent type,

meaning the flow is complicated and unstable. This instability is modeled in three ways [27].

The well-known Rayleigh instability happens at a low charging flux, giving the flow an axially symmetrical shape. The latter axially symmetric instability that is admitted as a transmission mode takes place at certain high electrical fluxes.

One other instability occurs during whipping, because of the ruffling in the field charge distributions. These instabilities align the polymer jet and cause a strain resulting with elongation of the fibers in cross-sectional area. The solution jet then follows a contoured space [34]. Once the contour is shaped, the jet keeps on twisting as much as possible; before it reaches the collector. Jet expansion occurs in this portion of the ejaculation [28, 33]. Then, the individual jet separates into numerous other sub-jets before they arrive on the collector screen. In this portion of the movement, the flux carried by per jet is the same, and dispersed equally thus leading a uniform radius in each fiber section. This induces the fibers to be fine and subtle. As stated before, the fibers accumulate on the screen and are mainly aggregated as nonwoven filaments [35].

Wannatong *et al.* stated in their article that, there are six major types of forces influencing the formation of nanofibers, during electrospinning [37]. They concurred that these forces are:

- Gravitational (or body) force
- Electrostatic forces affecting from atop the nozzle and to the collector screen
- Columbic force which is the main reason of the bending in the charged jet
- Visco-elastic forces, which acts in the opposite direction and attempts to minimize the effects of the Coulombic forces
- Surface tension induced forces
- Friction forces

In electrospinning, these parameters are grouped and examined in different topics.

The actual sub-classes of parameters are to be checked in the later sections of the research. As stated before, this research paces within the change of these parameters.

3.3. Parameters of Electrospinning

There are numerous parameters that and affect the fibers during the process. They can be classified in 3 arch-reasons:

- Polymer solution related parameters
- Process parameters
- Ambience related parameters

Conductivity of the solution, surface tension, dielectric effect, concentration of the solution and polymer chaining structure, volatility of the solvent –which means how easily the solvent evaporates), are the parameters based on the solution. Voltaic difference (applied voltage or the electrical potential), solution velocity (directly related to the mass rate), diameter of the nozzle, distance between the nozzle and the collector surface, and the geometry (or dynamicity) of the collector surface are the processing parameters.

Ambience related parameters can be expressed as the ambient temperature where process occurs, humidity, air velocity in the ambience, pressure, and atmosphere around [2, 13, 29, 33].

3.3.1. Polymer Solution Related Parameters

These parameters are the major parameters effecting on the morphology of the fibers produced. All sub-parameters shall be elaborately examined.

3.3.1.1. Conductivity of the Solution. Common solvents utilized in electrospinning process mainly inhene a very limited amount of free electrons roaming, thus their conductivity is

very limited. In electrospinning, the process can only be launched if the solution possesses sufficient charge to overcome the surface tension that holds the polymer solution still. Reciprocal repellent forces cause the polymer solvent jet to be tightened and this reciprocal repelling rises as the amount of charges on the jet surface rises.

Adding ions improves the conductivity. This improvement may help production of fibers without beads (as shown before) since tightening has increased and to some extent, a decrease in fiber diameter can be monitored. For example, electrospinning of a well-known polymer, Polystyrene (PS) has been researched in eighteen different types of solvents [38]. Finally, it has been found out that, type and conductivity of the solvent are major parameters in identifying the fiber morphology.

Solvents with reasonable conductivity values have been observed to be more eager to be electrospun, than those with zero conductivity. Chemically, it has been found out that, adding inorganic salts (i.e. NaCl, LiCl and MgCl₂) improves the conductivity of a polymer solution [39]. Once these additives are in the solvent, conductivity exhibits a monotonous rise, yet, the diameter of the resulting fibers is observed to be higher after addition. The major cause of this rise is the increase of the visco-elastic force in the solution. In contrast with inorganic salt additives, organic ones contributed to the shrinkage in the fiber diameter. Conductivity of the polymer solution was observed to increase swiftly with the addition of a small amount of salt, but the viscosity and the surface tension remained constant whereas viscosity and surface tension remained constant [40].

PAA (Polyacrylic acid sodium salt) and PAH (Polyallylamine hydrochloride) were combined to study the effect of electrolyte additive to poly (ethylene oxide) (PEO) based solutions [41]. Adding PAH and PAA triggered a rapid rise in the solution conductivity bringing an improvement in the fibers, which had become finer and straighter. Meanwhile, the effect of the solution conductivity upon morphology was not so influential. The diameter of the fibers underwent a limited shrinkage from 0.35 to 0.2 nanometers and this decrease kept under a threshold value since the nominal diameter of the fibers was not straight-related to the conductivity. Beaded fibers can be eliminated by addition of a small portion of

cationic surface active compounds (surfactants). Additive of these substances also increases the conductivity of the solution. This change can be observed from the increase in the nominal charge of the jet. This strengthens the bending of the jet during electrospinning of PS and UHMWPE [42].

As a conclusion, improvement of conductivity of the solution can be achieved by adding highly conductive liquid substances (i.e. solvents) or surface active compounds and also setting the Ph value of the solution.

3.3.1.2. Surface Tension. Complying with the definition of tension, surface tension is expressed as the force exerted upon the plane of the surface per length.

In electrospinning, the polymer solution must satisfy a threshold amount of charge to overcome the surface tension which restricts the spinning operation by forcing the droplet to adhere the nozzle. During the process, beaded fibers can be observed to form through the diameter due to the effect of the surface tension. As a remedy, there are many methods to reduce the surface tension value. The first method is to balance it using solvents with low surface tension characteristics. Beads were observed to grow in water/PEO solution [25]. Adding ethanol (C_2H_5OH) in the water/PEO solution greatly decreased the surface tension of the polymer solution and unbeaded, uniform PEO fibers were spinned.

The same effect was also studied by Fong *et al.* [43]. Fong and his team determined that, bead formation is highly effected by the value of surface tension. PVP (Polyvinylpyrrolidone) dissolved in N - DMF (normal - Dimethylformamide) triggered bead formation as they have high values of surface tension. Moreover, fine and smooth fibers without beads were spotted in PVP/Ethanol solutions, with less surface tension value.

Another effective method is to add surface active compounds which are highly likely to decrease the surface tension. Zeng *et al.* utilized indissoluble surface active compounds in their study [44]. On the other hand, adding miscible (thus, soluble) surfactants improved the rate of fiber formation, by minimizing the fiber diameter. However, indissoluble surfactants

were much more efficient at shrinking the diameter [42].

3.3.1.3. Dielectric Effect. Dielectric materials are materials that do not or very slightly conduct (insulation) electricity, yet, they promote electrostatic field effectively. In electrospinning, polymer solutions with higher dielectricity are favorable due to the reduction in bead occurrence and amendment in fiber morphology (i.e. finer fibers). The correlation between the diameter of the produced fiber and dielectricity of the solution were examined at the end of this research and it has been concurred that, fibers produced using solvents with higher dielectricity were finer in diameter [41].

The higher the dielectricity of the solution, the higher charge density is. This triggers an increase within the charges through the jet. The jet bends more easily if the charge flux is increased, beyond the electrical potential. This helps explain obtaining fibers with less beads and less diameter. Besides, utilizing a solvent with higher dielectricity boosts bending instability. Dielectricity has a prominent effect on fiber formation. The relation between fiber formability of the resultant fibers and dielectricity is exponential [37].

3.3.1.4. Viscosity, Concentration and Chain Entanglement. Viscosity is the reluctance to flow of a fluid. Many parameters influence the viscosity value of a fluid. The main factors are, molecular weight, chain entanglement, temperature of the liquid and concentration.

Molecular weight directly affects the viscosity. The same polymer having different molecular weight has different viscosities, the higher it is, the higher the other. Molecular weight has to have a suitable value to regulate the viscosity of the solution otherwise, fiber formation may not occur due to the lack of formation of continuous jets.

Continuous jets can only form under suitable chain entanglement conditions, which are directly related with the length of the polymer that is determined by the molecular weight of it. A secondary effect of entanglement is the formation of beads along the fiber. Shortly, the more the molecular weight, the more the chain entanglement and thus, the more viscosity and fiber formation.

Temperature of a fluid is also another major parameter on viscosity. Considering a honey, (a highly viscous and well known fluid) if it is kept in a fridge, it becomes less eager to flow, meaning more viscous. Otherwise –if kept in a warmer ambience- it is more easily to pour it into the bowl. Summarizing, the more the temperature, the less the viscosity.

Increasing the concentration of a solution is another way to increase the solution viscosity for it means the presence of polymer molecules increase in a volume. Increasing the concentration exhibits nearly the same way with increasing the molecular weight of the polymer. Concentration also influences entanglement. At higher levels of solution concentrations, viscosity increases, refraining bending instabilities. This results with accumulation around a smaller area with fibers having higher diameters.

At low levels of viscosity, chain entanglement diminishes and surface forces become more effective during spinning, and resultant fibers are more eager to have beads. On the other hand, at high viscosity levels, jets can bend totally and finer, un-beaded fibers form. This phenomenon can be seen in Figure 1.4.

High viscosity also causes the jet to separate into sub-jets that form finer fibers. Besides, feeding the polymer solution to the system becomes harder and dehydrating may be observed at the edge of the nozzle. Figure 3.3 illustrates resultant electrospun fibers with distinct viscosities.

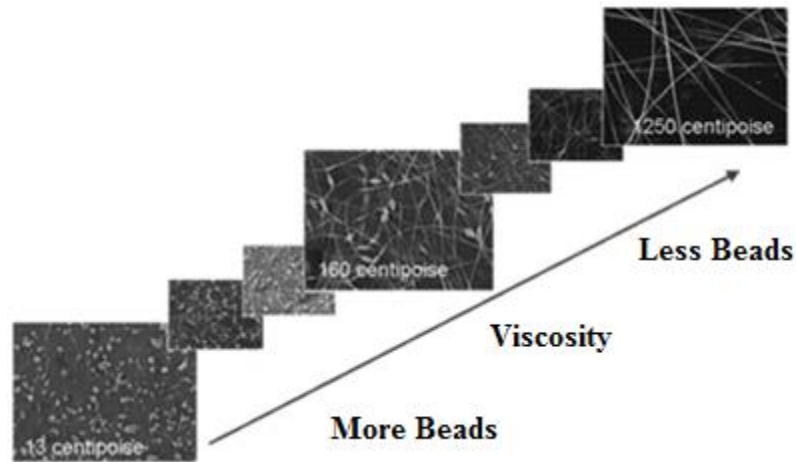


Figure 3.3. Change of bead formation with respect to viscosity [23].

In their research, Jarusuwannapoom *et al.* detected beads at low concentration intervals [38]. They figured out that, the more the concentration of the solution, the more the diameter of the resultant fibers and the less the bead formation along the fibers. It was also stated that, the nominal diameter of the resultant fibers has an exponential relation with respect to the viscosity [39]. This exponential equation is termed as:

$$d = 88.7 + 0.804 \exp(0.00137\mu) \quad (3.3a)$$

Where, d is the nominal fiber diameter in nanometer (nm) and μ is the dynamic viscosity in centipascal (cP), belonging the polymer solution utilized in the experiments.

It is specified that, if the viscosity of the solution is raised, so does the size of the beads, but the bead formation in the resultant fibers reduces. In the end, the morphology of the beads invert to needle-like shape from spherical shape [25]. During the research, it was also monitored that the bead density falls at high amounts of viscosity [45].

In another research, Koski *et al.* researched the effect of chain entanglement on fiber and bead formation [46]. It was found out that, more than 2.5 entanglements for each chain is suitable to form stable fibers. They also used six PVAs (Polyvinylalalanine) having different

molecular weights between 9×10^3 and 186×10^3 during the process and saw that, in per sample; a threshold concentration was needed to obtain stable fibers [47]. On the other hand, another result was concurred, which stated that, increasing the solution concentration ends with decrease in fiber density and resultant fiber morphology alters to flat from distorted.

3.3.1.5. Volatility of the Solvent. Another prominent aspect in electrospinning process is the volatility of the solvent. Because electrospinning is based on rapid evaporation of the solvent and adhering of the polymer onto the collector screen, volatility of the solvent affects the rate of evaporation of the solvent. Volatility contains sub-parameters that play role on it. They can be expressed as:

- Boiling point of the solvent
- Specific heat capacity
- Thermodynamic properties (i.e. enthalpy)
- Rate of the heat radiated from the supply
- Interaction of molecules in the solvent
- Surface tension
- Air aspiration above the liquid boundary [13]

Volatility of the solvent also plays an important role in determining the characteristics of resultant fibril forms produced via electrospinning. During the process, the solvent starts to evaporate just when it leaves the nozzle, until reaches the collector. To ensure fibrous structure, the solvent must evaporate before it reaches the collector. Beyond this, if the solvent retains on the collector, the resultant structure becomes wet fibers or thin rod-like films [13, 29]. It is also alleged that, volatility affects the formation of gaps, pores through the fibers [48, 49]. A reduce in volatility ended with finer fibre surfaces, yet, solvents having low boiling point are favourable due to the their improved evaporation. In their research, Matthews *et al.* preferred a volatile solvent with low points of boiling [50]. They concluded that, volatility of the solvent plays an important role on fibre morphology. Swift evaporation can trigger spiral, well routed fiber formation [31].

3.3.2. Process Parameters

Process parameters also play a role in the electrospinning process, yet, they are not as effective as polymer related ones. They can be admitted as exterior forces exerted upon the system.

3.3.2.1 Applied Voltage. Applied voltage is the main parameter which defines the rate of charge that flows through the system thus, it is taken as important. In the electrospinning, there is a threshold voltage after which electrostatic forces overcome the surface tension, resulting with the spinning mechanism to activate [50]. Threshold (or critical) voltage is directly related with the surface tension of the solution and are correlated in a linear manner [51]. The shape of the drop at the edge of the nozzle can be altered by raising the amount of the applied voltage. The more the applied voltage is, the more the charges passing through the jet are. Raising the charge triggers a speed-up in the jet and more solution can be spun. Raising the voltage also allows to obtain finer fibers, shrank in diameter. By supporting a high amount of charge with a highly-volatile solvent, even dry fibers can be produced. Under some conditions, with solutions lacking high amounts of viscosity, compensation with high voltage can cause multi-jet occurrence. By this way, finer fibers can be produced.

Bead formation is also highly dependant on the applied voltage. Mainly, the higher the voltage, the more beads through the fibers, yet, increased bending of jet results with fewer beads through the fibers [38]. At low voltage intervals, because of the poor electrostatic force, it may take longer for the fibres to travel from nozzle to the collector. This ensures obtainment of finer fibers. Wang *et al.* studied the correlation between the jet cone diameter and the fibre diameter and interpreted the influence of potential difference [52]. They found out that both the jet and the fibre diameter reduced slightly. On the other hand, an improved chain sequence was observed as voltage was increased. In another research, a relation between the voltage and diameter was obtained and it was stated that, fibers got coarser when the voltage is altered from 5 kilovolts to 25 kilovolts [53].

3.3.2.2. Feed Rate. Feed rate (or flowrate) is the parameter that expresses the amount of the solution ejaculated onto the collector per unit time. Fiber formation can be kept under control by altering the feedrate. It determines the shape and occurrence of the Taylor cone. Furthermore, it also plays role on bead formation and fiber shape. A raise in the flowrate may end with an increase in fiber radius and bead dimension. Simply; the more the feed rate, the more the amount of the polymer electrospun. This results with the need of more time for removing the excessively wet polymer on the collector as the solvent will not have sufficient time to evaporate and leave the sole polymer behind. Residue solvent can distort the fibrile structure and the result may be and undesired complex polymer structures, which make of no use.

3.3.2.3. Distance Between the Nozzle and the Collector. Another prominent parameter in electrospinning process is the distance for it determines how long and far the solution shall travel from the nozzle to the collector. If it is set too low, then the solution will lack enough time to evaporate from the polymer and wet solution accumulates on the collector. The result may be consolidated non-fibril polymers with distorted interface due to the residual solvent in the media whereas, short distances may trigger an increase in the magnitude of the electric field.

In the adverse case, when the fistance is kept longer, the solvent can find enough time to leave the solution and jet bending can occur before it arrives across yet, too much increasing also causes a drastic formation of beads and the value of the density [38].

In his research, Wang *et al.* studied the correlation between the distance and the diameter of the jet on Polystyrene (PS) and concurred that the distance and the jet diameter has an inverse relation [52].

3.3.2.4. Type of the Collector. The regular material used in electrospinning to collect the spun fibers on the collector is an insulator and is mainly a piece of aluminium foil for it is a highly qualitative conductor material. The reason why conductive materials are used on the collector is that they help maintain the voltaic stability between the nozzle and the collector.

Otherwise, the fiber formation may be disrupted and the process can fail. Conductive materials also lure more jets, which mean an increase of the fiber deployment on the collector. Porous or non-conductive materials can be used as on-collector gatherer but the result may be non-aligned fibers, like combs heavy intersections.

On the other hand, rotating disks or moving surfaces can be utilized, too. This triggers the aligned fiber formation mechanism and resultant fibers become finer. Although it sounds more favourable, it is not applicable to all types of solutions for it requires higher surface tension to adhere the rotating media.

3.3.2.5. Nozzle Diameter. Another important aspect to interfere the fiber parameters in electrospinning is the nozzle diameter for it plays a prominent role in ejaculation speed and feed rate. As expected, a reduction in the nozzle diameter ends with higher speed. This causes a significant decrease in:

- Coagulation
- Formability and Density of the Beads
- Fiber Diameter

A reduction in the nozzle means an increase in the surface tension that holds the polymer on the nozzle, preventing ejaculation and thus, spinning. In accordance with this, more electric charge is required to force the droplet to leave the nozzle. In case the charge is not tuned to a higher value, the polymer will be able to find more time to release its solvent (evaporation) and accumulate on the collector. However, too much decrease in the nozzle diameter is not a desired change as it prevents the formation of droplets more and more [13]. Zeng *et al.* researched three distinct capillary effect of the changing of the diameter and concluded that, increasing the nozzle diameter triggered a rise in the voltage to overcome the threshold value and expansion of the fibers along the diameter, ending with coarser fibers [56].

3.3.3. Ambience Related Parameters

Ambience related parameters still remain unclear for there have not been too much studies made on it. The process is heavily related to the ambient parameters like the air pressure, moisture and temperature.

3.3.3.1. Ambient Temperature. Since temperature is a dominant parameter on viscosity and evaporation time of the solvent, it also affects the process quite a lot. In warmer ambiances, the solvent can be disposed off the polymer much easily than cooler ones. On the other hand, less viscous polymers -due to the warmer environment- can be spun quicklier and formation of finer fibers is assured. High temperature levels also triggers chain formation in the polymer [56].

3.3.3.2. Moisture. Higher humidity comes along with more water droplets in the air and can cause osmosys and drill pores along the polymers, especially when more volatile characted solvents are used. The higher the humidity, the higher the amounts of damp and so are the rate of pore formation. According to the research made by Casper *et al.* the data are given in the Table 2 [57].

Table 3.1 Changing of pore diameters with respect to the moisture rate [57].

Moisture range (percentage)	Range of the Pore Diameters (nm)	Nominal Pore Diameter (nm)
31-38	60-190	85
40-45	90-230	11
50-59	50-270	115
66-72	50-280	135

Moisture where electrospinning is performed has a significant effect on fiber morphology for it directly triggers pore formation, especially if highly volatile solvents are used. Another important parameter that moisture is directly related to is evaporation rate. In

higher moisture levels, evaporation of the polymer solution gets harder. This eventually leads to wet-fiber disposal upon the collector, causing a distortion in the resultant structure.

3.3.3.3. Ambient Pressure. The influence of the pressure to the process can be expressed in two sub topics of which first is the case when the pressure is lower than the atmospheric pressure values. Under these circumstances, the polymer solution in the feeder is more prone to expansion in blister forms and may not be suitable for the operation because of the prevention of the charge from meeting the polymer [13, 58, 59]. To overcome this effect, if the solution feedrate is tuned to a higher value, the operation may result with wet fibers [56].

3.3.3.4. Ambient Gas and Air Circulation. Altering the air conditions and surrounding gas may have influential effect in the electrospinning operation. Like in gas filled bulbs, different atmospheric gases exhibit different behaviors under an electric field. For example, if the process is held under helium atmosphere, a total fail occurs because of the breakup of Helium. Use of another fluid, CFC Fr - 12, causes the fiber diameter to be twice than it is electrospun in the air. Also, CFC Fr - 12 causes the fibers to sub-branch from the master fibers [13, 60].

Another atmospheric gas, SF₆ (Sulphur Hexaphloride) was studied by, Greiner and Wendorff during electrospinning of PA (Polyamide). Resultant fibers of 900 nm were obtained, which can be counted as very fine fibers [61]. Air circulation is another prominent parameter pending further data [62].

3.4. Materials Used in the Process

3.4.1. UHMWPE

Ultrahigh-molecular-weight polyethylene (UHMWPE) is a linearly branched very high density polyethylene (PE) having a molecular weight (M_w) between 2.3×10^6 and 16.3×10^6 Daltons ($1 \text{ Da} = 1.660538921 \times 10^{-27} \text{ kg}$). It has a unique compound of both physical and chemical properties and inheres the highest abrasive resistance of any thermoplastic

material, unusually high impact strength even at very low temperatures, a very low friction coefficient and high lubricative properties. Besides, it has unique dielectricity and stability for electrospinning [69]. Chemical structure, properties and mechanical properties of UHMWPE are shown in Figure 3.4 and Table 3.2.

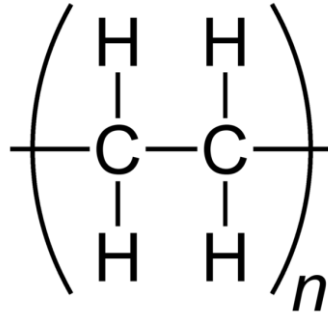


Figure 3.4. Structure of a UHMWPE mer

Table 3.2. Chemical and mechanical properties of UHMWPE [70].

Property	UHMWPE
Molecular Weight (10^6 g/mole)	3.5–7.5
Density (g/cm^3)	0.945
Melting Temperature ($^{\circ}\text{C}$)	132–138
Poisson's Ratio	0.46
Specific Gravity	0.925–0.945
Tensile Modulus of Elasticity (GPa)	0.5–0.8
Tensile Yield Strength (MPa)	21–28
Tensile Ultimate Strength (MPa)	39–48
Tensile Ultimate Elongation (%)	350–525
Impact Strength, Izod (J/m of notch; 3.175 mm thick specimen)	>1070 (No Break)
Degree of Crystallinity (%)	39–75

UHMWPE can be produced with various ways like melt solution spinning, sol-gel

process, melt deformation and electrospinning [71, 72]. The most palpable data has been acquired via spinning of gel particulates of UHMWPE [73]. UHMWPE can be processed through three steps, beginning from a UHMWPE ased solvent, resulting with fine and tough fibres. The first step comprises crystallization of the polymer to form single crystals as much as possible. After this, the second step which is based on formation of patterns in fibrile crystalline manner (shish kebabs) is applied [UHMWPE]. The final and the most important step is the drawing of the resultant fibres to obtain evenly-distributed and ultra strong crystals [74].

Today, super-strong and ultra-tough UHMWPE fibres are manufactured by a method inaugurated in 1984 [75]. In this method, a well-agitated solution of UHMWPE (ratio varies 2-10 wt %, solubility of the solvent and UHMWPE must comply or be close) is drawn in high temperatures like 150-160 °C such that the polymer can form intermediate-products, which are fibrile scaffolds. These intermediate-products must be drawn in a ratio varying from 4-30 [UHMWPE]. The final approximate mechanical properties of these fibrile structures are mainly: a tensile strength of 1.5 GPa, a Young Modulus of 140 Gpa, and a tensile strain of 0.2% [75].

So far, the most palpable research on electrospinning of UHMWPE was performed by Rein *et al.* in Israel Institute of Technology by 2006. Before this research, electrospinning of a highly-dense Polyethylene (PE) was declared [76]. The mechanical properties of the resultant scaffold fibres came close to medium-patterned polyethylene were $\sigma_t \approx 1$ MPa and $E \approx 60$ Mpa [76].

This research was performed to manufacture fine UHMWPE nanofibers, but as a difference from previous (and scarce) studies, it has utilized a new co-polymer, Butyl Rubber, to mix with UHMWPE.

3.4.2. Butyl Rubber

Butyl rubber is a sort of inorganic, artificial rubber. It is expressed as an elastomer,

which inhere very high elastic/plastic strains. Butyl rubber is synthesized by polymerizing approximately 97 wt% isobutylene and 3 wt% of isoprene. The resultant polymer is PIB (polyisobutylene), which is highly leakproof [78]. The density of butyl rubber is 0.863 g/cm^3 . The chemical bonds and structure of butyl rubber polymer, where n is the polymerization coefficient, is provided in Figure 3.5.

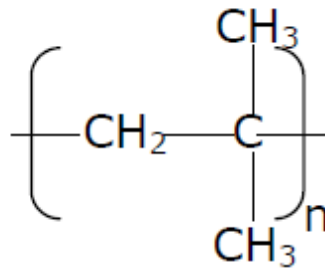


Figure 3.5. Chemical structure of a butyl rubber mer.

Butyl rubber has been electrospun only few times. One wide research on electrospinning of butyl rubber was performed by Göktaş [79]. Due to its compatibility in chemical wear coating applications and favourable mechanical properties, it suggests itself as a good option for electrospinning. A prominent research on butyl rubber was performed by Viriyabanthorn *et al.* They studied the importance of carbon addition parameters on the shape of the resultant fibers [80]. In their research, four distinct sorts of carbonic loading were applied on the polymer which was solved in THF (tetrahydrofuran). In the research, well-distributed fibers were rarely acquired in the absence of carbon addition in the solution. The team concurred that, the more the amount of carbon in the solution, the less beads and more formability of the fibers. Another study on effects of carbon addition during the electrospinning of butyl rubber was performed [81]. In the research, butyl rubber toughened with sulphur was mixed with different weight percentages of carbonic components, solved in THF. The solution was ejaculated at a rate of 1 milliliter per minute and fibers were collected on the drum screen. Finally, it was found out that, further addition of carbonic matters triggered a decrease in the fibre diameter, by reducing the viscosity and the electrical conductivity of the solution.

Butyl rubber was preferred to be mixed with UHMWPE due to its close chemical properties with it and was presumed to form a good reinforcement for the resultant fibers.

3.4.3. Tetrahydrofuran (THF)

The solvent is tetrahydrofuran, which is highly soluble with UHMWPE and butyl rubber. The chemical structure and properties are provided in Figure 3.6 and Table 3.3.

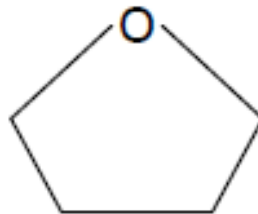


Figure 3.6. Chemical structure of Tetrahydrofuran [THF].

Table 3.3. Chemical properties of Tetrahydrofuran [THF] [81].

Chemical Property	Value
Density (at ambient temp, g/cm ³)	0.882
Molecular Weight (g/mol)	72.43
Melting Point (at sea side, °C)	-108.5
Boiling Point (at sea side, °C)	65.5
Viscosity (at ambient temp, (Pa.s)	0.48 x 10 ⁻³

3.5. Experimental Procedure

3.5.1. Preparations of the Solutions

UHMWPE was bought from Sigma Aldrich, with serial number 429015-250G in 2 items. When it came, UHMWPE was stocked in two 250 g polyethylene bottles and was in powder state and weighed approximately 224 grams when weighed in each bottle which was later weighed to be 26 grams.

On the other hand, Butyl Rubber was bought from Pro's Chemical Inc. with serial number J3300-Polyisobutylene. The product came in two 500 ml glass bottles in liquid state, as colorless as water. Because Butyl Rubber must contain 97 wt% Polyisobutylene solved in 3 wt% Isoprene as described in Experimental section, some Isoprene was required to solve it therein so, the Isoprene needed was bought from Sigma Aldrich with serial number I19551-500 ml. It was bottled in a 500 ml red sure seal bottle and was in powder state.

Finally, the solvent THF was bought from ESP Chemicals with serial number T5113 and arrived in a sure seal container and colorless as water.

As the polymers and the solvent were ultimately obtained, deciding how to evacuate them from their bottles and mixing were the challenges that were met. Initially, due to the scarcity of these valuable polymers, some preliminary experiments were decided to be made with very limited amounts to determine the electrospinning parameters between which they give good results. At this point, it was decided to electrospin each polymer in THF with surfactant NaCl, with different parameters when one single syringe was connected to the system at one experiment, to avoid unnecessary wasting of them. In consistence with this, the amount in a syringe that was exposed to electrospinning was decided to be 20 gr for each experiment. The weight ratios for each substance in per experiment were decided to be the following, in consistence with the weight ratios stated in the sources 26, 27, 28, 29, 30, 79, 80, and 81.

- UHMWPE : 12%, 15%, 20%
- BR: 6%, 12%, 18%, 22%, 25%
- NaCl: 1% (in all solutions)

At this point, the preparation of the first polymer, Butyl Rubber started. In order to achieve this, a total reserve of 20 gr of Butyl Rubber was decided for preparation, referring to the weight ratios above, for the initial experiments because a 20 gr of solution with the

Butyl Rubber weight percentages given above would total:

$$20 \text{ gr} * (6\% + 12\% + 18\% + 22\% + 25\%) = 18.6 \text{ gr} \quad (3.5a)$$

For Butyl Rubber inheres 97 wt% Polyisobutylene and 3 wt% Isoprene, 19.4 grams of Polyisobutylene and 0.6 grams of Isoprene were needed. For it was in liquid state, Polyisobutylene was poured from one of the bottles in which it was purchased, into 100 ml glass sample container in the desired weight which came 19.4 grams after slowly addition by a vacuum pipette. During this, the container was positioned on a digital weighing machine after the tare weight of it was entered. The sensitivity of the weighing machine was 0.001 gram.

Just then, Isoprene was prepared to mix with Polyisobutylene to form the ultimate Butyl Rubber that would be electrospun. To achieve this, the initial Isoprene bottle was opened and a little amount of the content was sucked into another vacuum pipette. After this, the Isoprene droplets were started to be poured into the glass sample container that was filled with 19.4 grams of Polyisobutylene in the previous step. The final weight displayed in the weighing machine was 20.00 grams with sensitivity 0.001 gram. Finally, this solution was positioned on a stirrer and was stirred for 2 hours on a digital flywheel magnetic stirrer that was set to 700 rev/min, to guarantee the mixing. The vacuum pipettes were cleaned using ethanol, by sucking it into them and waiting for 1 hour. During the experiments, as any of the stirring operation was over, the stirrer bar in the solution was removed with a pair of stainless steel tweezers.

By the time the stirring of Butyl Rubber started, the preparation of UHMWPE had begun. UHMWPE and THF had to be mixed as homogeneous as possible before they were sucked into the syringes. Apart from Polyisobutylene, Isoprene and THF, UHMWPE had come in powder state. Although it could have been dissolved in THF easily with the size of the powders in the bottle it arrived, and with the same calculation manner as that of Butyl Rubber's, 10 grams of UHMWPE were decided to be smashed manually in plastic garlic muller for 5 minutes to ensure a more effective mixing, after it was weighed in a plastic

sample container. After the operation, the smashed powder was kept in the same sample container of which lid was closed. UHMWPE was now ready.

As the stirring operation of reserve Butyl Rubber continued, the reserve UHMWPE was decided to be mixed with THF to initiate the experiments, so it was now the time to add THF in the prepared UHMWPE powders. Because THF arrived in its sure seal package in liquid form, it would have easily been added using the same vacuum pipettes that were cleaned with ethanol after usage.

The reserve NaCl was easily prepared by using a pack of commercial salt and smashing optically enough amount of it in the same garlic muller for another 5 minutes. The smashed NaCl powder was put in a plastic sample container.

3.5.2. Preliminary Electrospinning Experiments

The first preliminary experiment with UHMWPE was picked to be performed with 12 wt% of 20 gr, which meant 2.4 grams of UHMWPE was needed. From the reserve powder of UHMWPE, 2.4 grams of powder was put in a glass container and 0.2 gram of smashed NaCl was added on it afterwards. Finally, this mixture of the two powders was poured into the THF solution that weighed 17.4 grams. During weighing, the tare weight of the container was added into account.

Before this raw solution could be electrospun, it had to be exposed to a stirring operation to ensure a homogeneous solution as much as possible. To achieve it, the container that had the solution was stirred in the same stirrer for another 2 hours at 700 rev/min. When it finished, the solution in the container was totally sucked into a 25 ml syringe and was positioned on the electrospinning pump unit after it was connected to a polyethylene cable of which end was attached to the nozzle. The syringes were purchased from a pharmacy and were of single-use. The filled injectors are ensured to be safe by closing the safety clip on the pump.

The flat collector surface was also covered with a commercial aluminum foil to facilitate the removal of the collected fibers thereon.

At this crucial point, the other parameters –distance, rate and voltage- had to be adjusted. It was decided to alter the parameters manually during the process and detect the most stable flow of the solution optically. So the test started with 100 mm distance, 10 kV voltage and 1.5 mm³/s, the optimal process parameters.

Under these circumstances, the polymer drops were seen to be very eager to drop down the nozzle because of both low rate and voltage because of a great accumulation of polymer solution down the nozzle. This had two causes:

- The voltage was too low
- The viscosity was too high due to high weight percentage of THF

To overcome the first problem, as the experiment continued, the rate of the pump was altered to 1.0 mm³/s and a limited recovery at dropping was seen, yet with very wide, unstable and shattered ejaculation geometry onto the surface even without forming a Taylor Cone, due to the reasons mentioned above. That is why, firstly the voltage was gradually increased to 15 kV during spinning and the ejaculation geometry was seen to have recovered to a more, yet not totally, stable cylinder. After 7 minutes, having nearly half of the syringe consumed, the mechanism was shut down safely and the aluminum foil on which the spun fibers were ejaculated was removed by hand and disposed. Then a new aluminum layer was put onto the surface to repeat the experiment with the following data: 12 wt% UHMWPE in a distance of 100 mm, voltage of 15 kV and rate of 1.5 mm³/s. To overcome the viscosity problem, this preliminary experiment was repeated for 15 wt% and 20 wt% UHMWPE, word for word, and step by step with the same process parameters (100 mm, 15 kV, 1.5 mm³/s) as it was made for 12 wt%. As a difference, 15 and 20 wt% UHMWPE exhibited the following geometry and structure of the flowing behavior. These were the main criteria how the parameters were

determined.

- 15 wt% : A tangling and unstable Taylor Cone, more stable flow geometry
- 20 wt% : Stable Taylor cone

3.5.3. Results of the Preliminary Electrospinning Experiments

All these preliminary experiments were performed to see the morphology of UHMWPE fibers under the same conditions and determine the suitable interval of parameters. When each experiment was over, the aluminium foils on which the spun polymer layed was removed in a circular pattern via a stainless steel kitchen knife and was put in a plastic sample container, to be photographed under SEM.

The SEM utilized was ZEISS EVO MA 10- Tungsten filamented and had 500 – 30 kV voltage supported with SE, BSE, EDX and VPSE.

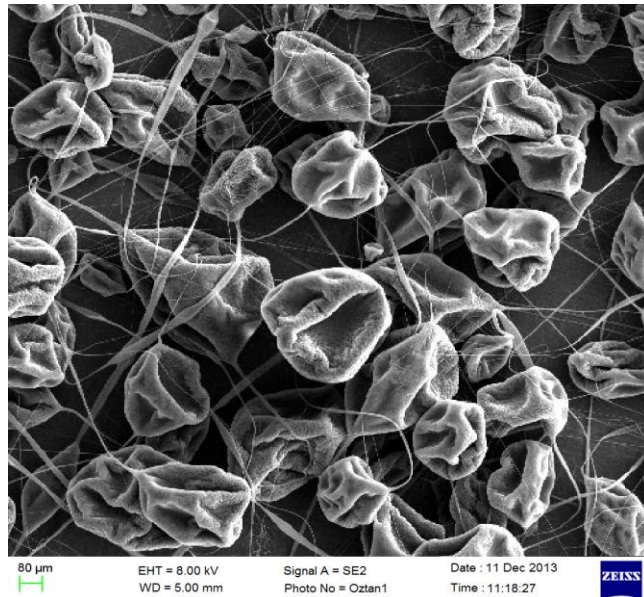


Figure 3.7. SEM image of 12 wt% UHMWPE.

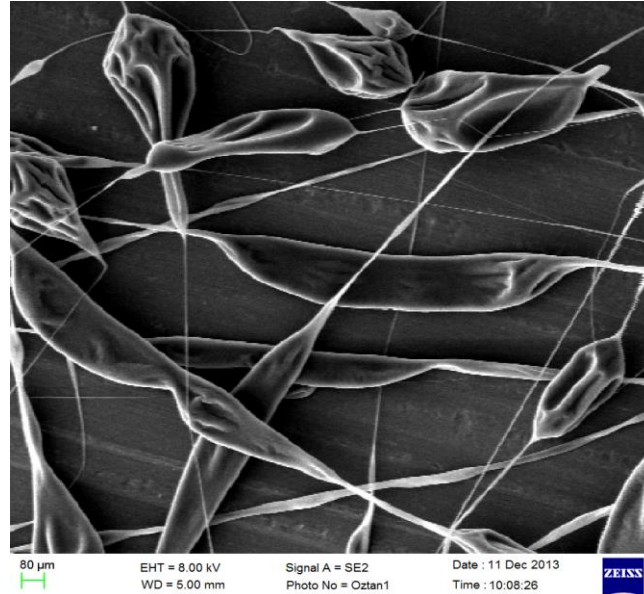


Figure 3.8. SEM image of 15 wt% UHMWPE.

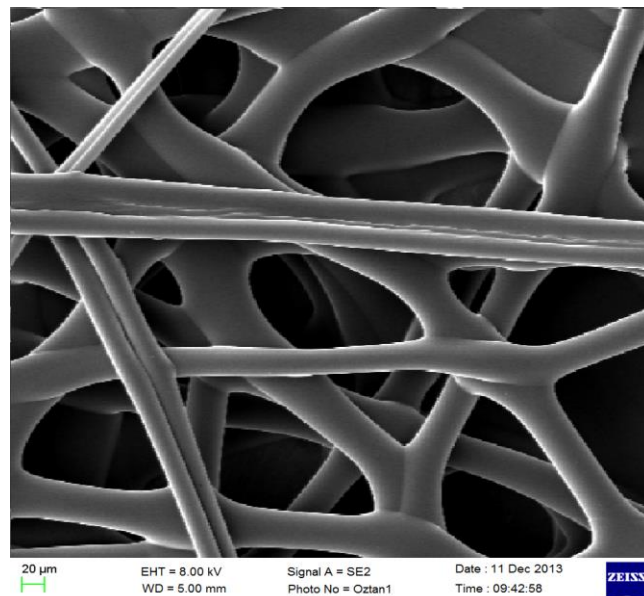


Figure 3.9. SEM image of 20 wt% UHMWPE.

According to these images, it can be inferred that:

- Under constant process parameters, the diameters of UHMWPE fibers tend to shrink

when weight ratio is increased.

- The less the weight percentage of UHMWPE, the more the viscosity forces that cause the beading which can be seen from the images.

Having learned about the initial information about the optimum parameters of electrospinning for only UHMWPE, it was now time to determine the same parameters and compare the morphology of Butyl Rubber samples with those of UHMWPE, with different weight percentages. Because the components of Butyl Rubber, Polyisobutylene and Isoprene were more in the stock, than UHMWPE, the weight ratio parameter was expanded to a bottom limit of 6 and upper limit of 25 to determine the optimum weight ratio with respect to the morphology of the samples. On the other hand, the process parameters were also kept the same (100 mm, 15 kV, 1.5 mm³/s, 20 grams of solution in single syringe) as the preliminary experiments done with UHMWPE in order to make a second comparison between these polymers.

For this, the recently-stirred Butyl Rubber sample was mixed with 1 wt% NaCl as 6, 12, 18, 22 and 25 wt%. A second 2-hour stirring with 700 rev/min was also performed when THF was added to each sample.

As soon as the stirring operations were over, the mixtures were sucked into the 60 ml syringes in all experiments, to avoid any unexpected coagulation or precipitation. So, the Butyl Rubber mixtures were subjected to electrospinning just as they were sucked in the syringes, too. The first Butyl Rubber sample with 6 wt% was prepared as follows:

- The amount of Butyl Rubber in the syringe = 1.2 gr
- The amount of NaCl in the syringe = 0.2 gr
- The amount of THF in the syringe = 18.6 gr

All these weighing operations were performed the same way as UHMWPE, and the setup was prepared with the same process parameters as UHMWPE, which are a distance of 100 mm, voltage of 15 kV and rate of $1.5 \text{ mm}^3/\text{s}$. This was decided because of the proximity of the viscosities of these two polymers which will play the main role once the process parameters are fixed [70, 78]. During the experiments made for each of the Butyl Rubber solution, the conditions of Taylor Cone and ejaculation are as follows:

- 6 wt% Butyl Rubber: Highly unstable Taylor Cone formation due to the crossings in flow geometry and rapid dropping down the nozzle.
- 12 wt% Butyl Rubber: More stable Taylor Cone formation yet, unstable flowing dropping which is less than 6 wt%.
- 18 wt% Butyl Rubber: Almost stable Taylor Cone formation and stable flow. Taylor Cone shooke for a few degrees during spinning.
- 22 and 25 wt% Butyl Rubber: Clearly stable Taylor Cone formation and stable flow. All seemed quite fair.

In conclusion with all these experiments, it was inferred that Butyl Rubber exhibits the same behavior as UHMWPE: The more the weight percentage, the more stable flowing conditions. Once the preliminary Butyl Rubber experiments were over, it was not taken as crucial to get the SEM images of the samples because the process parameters and the spinning behavior were exactly the same as each other.

After these operations, it was now time to launch the main experiments in which the polymers shall be ultimately mixed and the electrospinning behavior was to be inspected along with the morphology of the spun fibers. Mixing of the two polymers can be performed by two ways.

Conventional mixing, like in preliminary experiments, the polymers and the solvent can be blended in a container and then sucked into one single syringe that shall be connected to the pump and perform the spinning. This method was not preferred mainly because the volume of the polymer mixture would exceed a maximum of 25 ml by twice and would require a much bigger syringe, which would complicate the connection to the pump. On the other hand, obtaining such a big sized syringe would be difficult compared to the little ones utilized in the preliminary experiments. Also, if the operation might have delayed somehow, this method might cause material wasting due to congelation in the syringe because of long time elapsed.

Dual syringe mixing that involves the mixing of the polymers that were fed through two distinct syringes connected to the same pump. The mixing occurs in the multi-inlet nozzle to which the syringes are connected via polyethylene cable. This method was suitable because it eliminates the disadvantages of the conventional method. As a drawback, it requires two syringes so, is more expensive. During these main experiments, the preparation operations are performed exactly, step by step the same way as the preliminary experiments. The minor differences are the connection of both syringes onto the pump at the same time and the synchronization of the ending of the stirring times to spin them when are as homogeneous as possible. On the other hand, the major difference is that the weight percentage of UHMWPE was fixed to 20% in all experiments to determine the behavior of the altering Butyl Rubber weight percentage with respect to the constant one of UHMWPE. This was decided because the electrospinning behavior of Butyl Rubber was more predictable referring to the results of the preliminary parameters. As stated there, Butyl Rubber exhibited similar behavior even under distinct weight percentages like 18, 22, and 25. On the other hand, UHMWPE exhibited a less predictable behavior for weight percentages of 12, 15, and 20, of which 20 wt% was the suitable one. All these reasons compel to fix the weight percentage of UHMWPE to 20.

3.5.4. Experimental Setup

The setup utilized in the process is as illustrated in Figure 3.10.

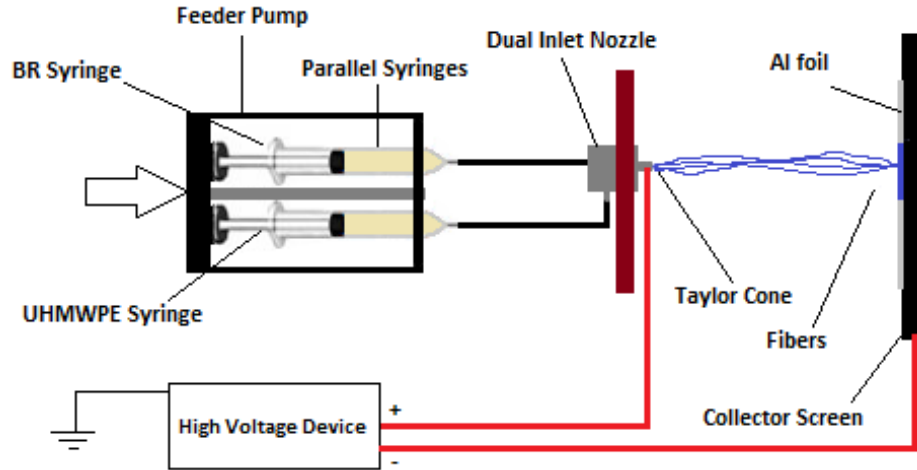


Figure 3.10. Illustration of the test equipment used in the experiments.

The device utilized has two syringes which are connected to a nozzle with dual inlets. The screen is covered with an Aluminum foil to facilitate the removal of the fibers. The positive edge of the alligator - clipped high voltage cable is attached to the tip of the nozzle whereas the negative side is attached to the collector screen to form the electrical field needed to spin the solution. Finally, the high voltage device is grounded to the soil with a copper stick. Finally, the illustration of the dual - inlet nozzle is provided in Figure 3.11.

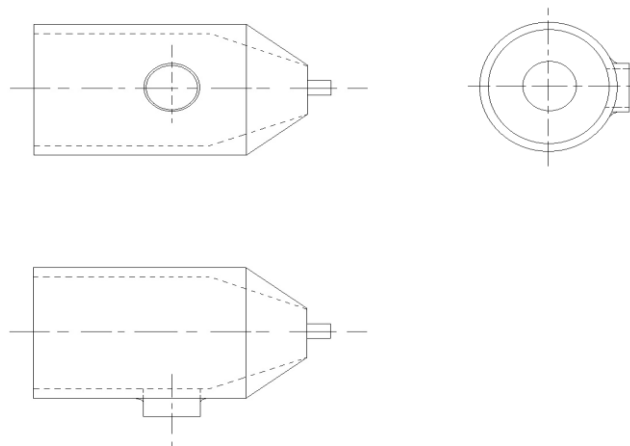


Figure 3.11. Illustration of the dual – inlet nozzle used in the experiments

3.5.5. Investigated Parameters

Three of the aforementioned parameters were studied in the experiments. The process was performed under constant ambient conditions (1019 hPa ambient pressure, 22 °C temperature).

The solvent and the polymer were mixed also in the ambient temperature, to keep the viscosity forces high and the voltage requirement low. Table 3.4 given below summarizes the values and the types of the parameters altered during each experiment. The results of a total of 18 experiments are reported in the results section.

Table 3.4. Summary of the parameters altered in each experiment.

Applied Voltage (kV)	wt% (BR/UHMWPE)	Feed Rate (mm ³ /s)	Distance (mm)
10	25/20	1.65	100
	22/20		
15	25/20		
	22/20		
20	25/20		
	22/20		
Distance (mm)	wt% (BR/UHMWPE)	Feed Rate (mm ³ /s)	Applied Voltage (kV)
80	15/20	1.3	15 kV
	18/20		
100	15/20		
	18/20		
150	15/20		
	18/20		
Feed Rate (mm ³ /s)	wt% (BR/UHMWPE)	Distance (mm)	Applied Voltage (kV)
0.83	15/20	100	15 kV
	18/20		
1.3	15/20		
	18/20		
1.65	15/20		
	18/20		

4. RESULTS AND DISCUSSIONS

This chapter contains the images of the electrospun fibers taken under SEM, and the correlation of the parameters varied during the experiment process.

4.1. Applied Voltage

The first process parameter that was examined is the influence of the voltage applied on the system. For this, the other two parameters – distance and feed rate – were kept constant at, by turn, 100 mm and 1.65 mm³/s. Afterwards, the applied voltage was set to three values; 10, 15 and 20 kV; and finally, the operation was performed. After receiving the SEM images, it could be stated that the fiber dimensions decreased by increasing voltage. Figure 4.1 and 4.2 provide the SEM images of the resultant fibers.

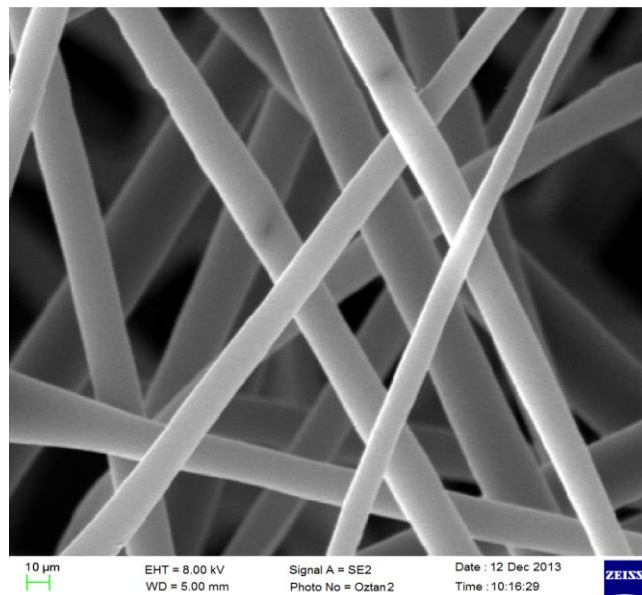


Figure 4.1. SEM image of 25/20 wt% (BR/UHMWPE) electrospun under 10 kV.

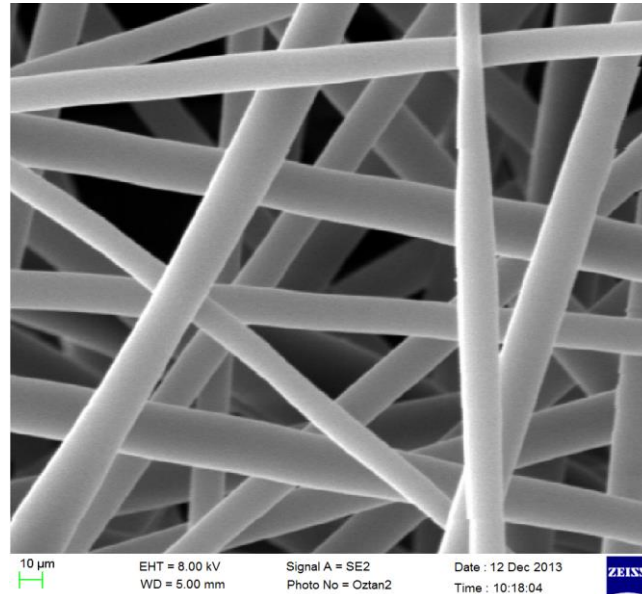


Figure 4.2. SEM image of 22/20 wt% (BR/UHMWPE) electrospun under 10 kV.

Summarizing the images provided above, Table 4.1 gives the correlation between the solution types and fiber diameters.

Table 4.1. Correlation of concentration and fiber diameter electrospun under 10 kV

Solution Type	Nominal Fiber Diameter (μm)
wt% 25/20 (BR/UHMWPE)	10.30 ± 2.00
wt% 22/20 (BR/UHMWPE)	12.20 ± 2.10

As for the operations performed under 15 kV with two different solutions, the SEM images are provided in Figures 4.3 and 4.4.

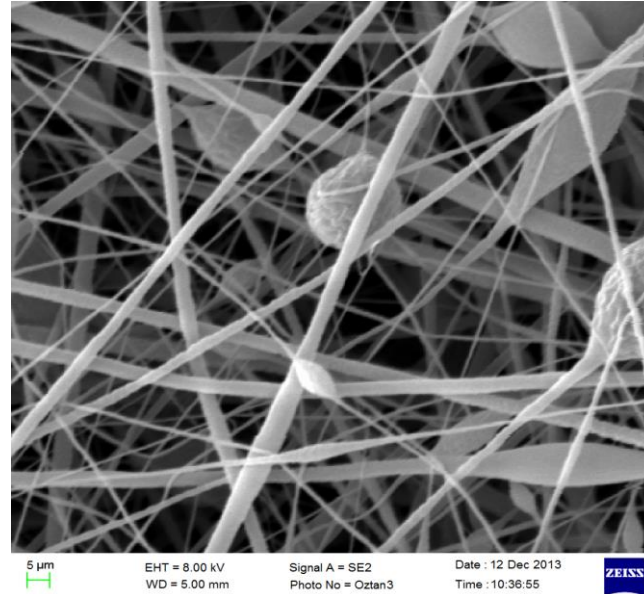


Figure 4.3. SEM image of 25/20 wt% (BR/UHMWPE) electrospun under 15 kV.

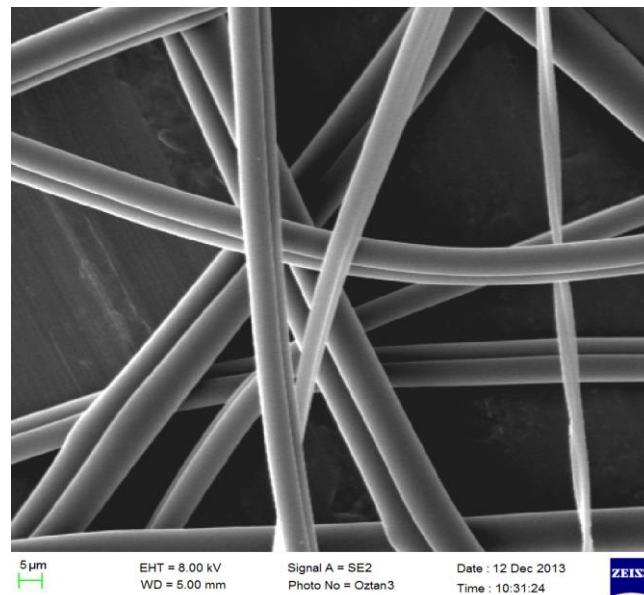


Figure 4.4. SEM image of 22/20 wt% (BR/UHMWPE) electrospun under 15 kV.

In the same manner, summarizing the two images provided above, Table 4.2 gives the correlation between the solution types and fiber diameters.

Table 4.2: Correlation of concentration and fiber diameter electrospun under 15 kV.

Solution Type	Nominal Fiber Diameter (μm)
25/20	4.30 ± 1.30
22/20	7.20 ± 2.10

The final solutions exposed to electrospinning under 10 kV exhibit the following morphology, they are given in Figure 4.5 and 4.6.

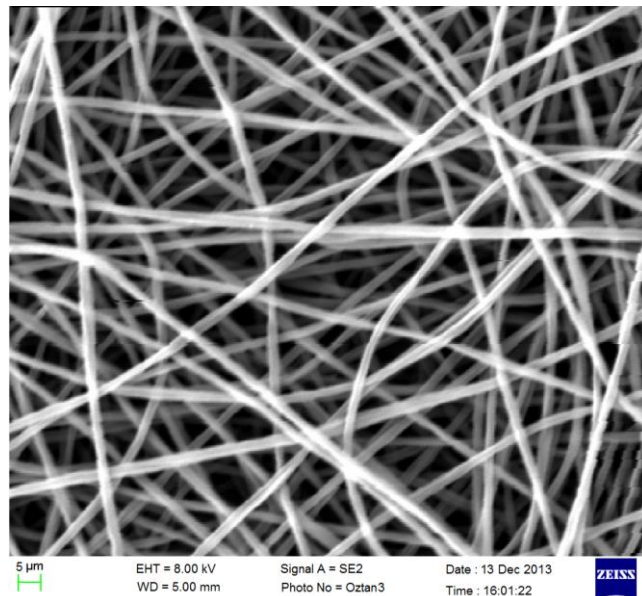


Figure 4.5. SEM image of 25/20 wt% (BR/UHMWPE) electrospun under 20 kV.

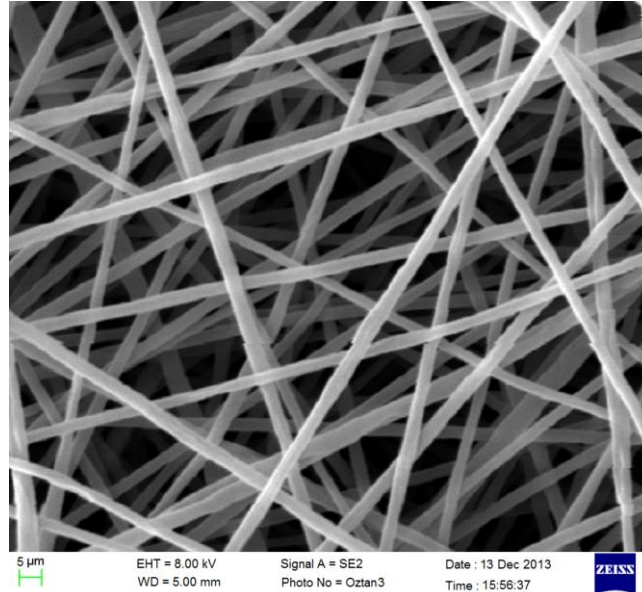


Figure 4.6: SEM image of 22/20 wt% (BR/UHMWPE) electrospun under 20 kV.

These results are summarized in Table 4.3.

Table 4.3. Correlation of concentration and fiber diameter, spun under 20 kV

Solution Type wt% (BR/UHMWPE)	Nominal Fiber Diameter (μm)
25/20	2.40 ± 0.60
22/20	3.20 ± 0.80

4.2. Distance between Nozzle and Collector

The second parametric analysis was performed to see the results of altering the distance between the nozzle and the collector. To see the effects, the other two parameters, applied voltage and feed rate were kept constant at, namely, 15 kV and $1.3 \text{ mm}^3/\text{s}$. The varying parameter, distance was adjusted to 80, 100 and 150 mm. The polymer solutions used in the processes are 18/20 (BR/UHMWPE) and 15/20 (BR/UHMWPE). Figures 4.7 to 4.12 illustrate the morphologies.

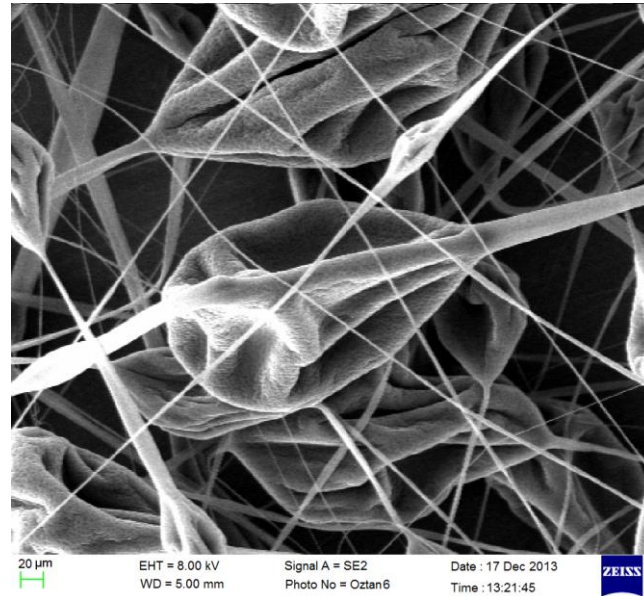


Figure 4.7. SEM image of 18/20 wt% (BR/UHMWPE) electrospun at 80 mm.

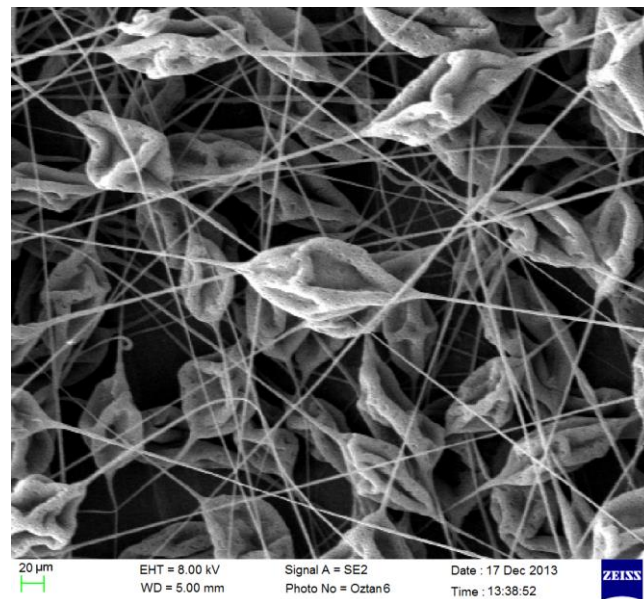


Figure 4.8. SEM image of 18/20 wt% (BR/UHMWPE) electrospun at 100 mm.

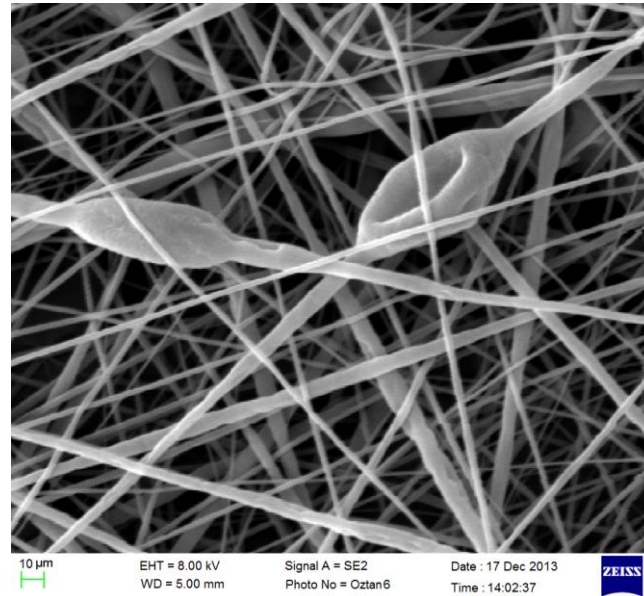


Figure 4.9. SEM image of 18/20 wt% (BR/UHMWPE) electrospun at 150 mm.

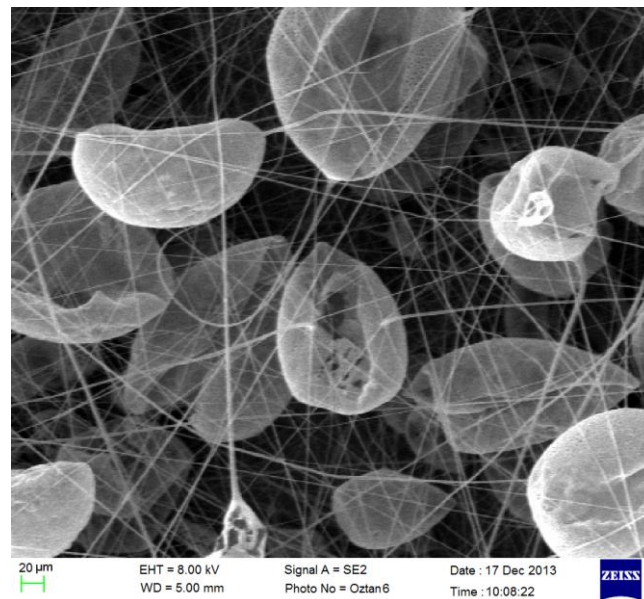


Figure 4.10. SEM image of 15/20 wt% (BR/UHMWPE) electrospun at 80 mm.

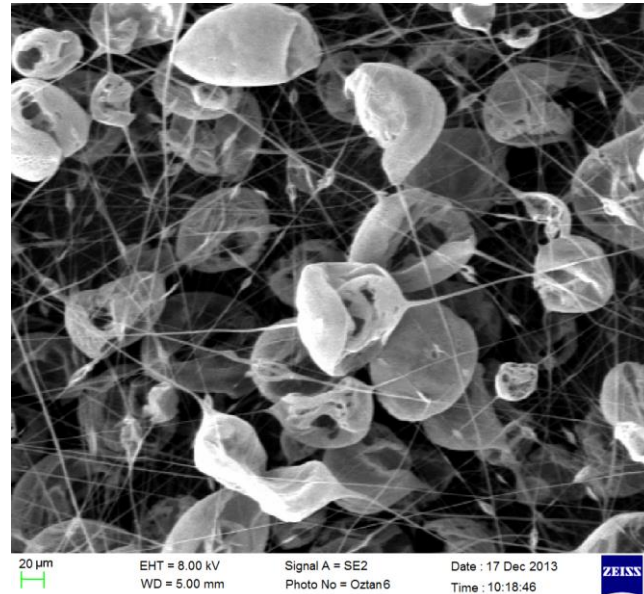


Figure 4.11. SEM image of 15/20 wt% (BR/UHMWPE) electrospun at 100 mm.

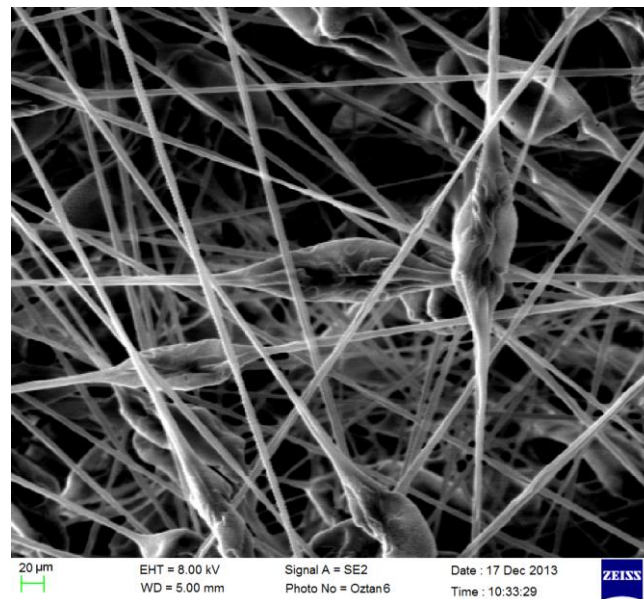


Figure 4.12. SEM image of 15/20 wt% (BR/UHMWPE) electrospun at 150 mm.

In accordance with the SEM images provided above, the nominal fiber and the nominal bead diameters are provided along with the process in Table 4.4.

Table 4.4. Correlation of Concentration, Distance, Fiber and Bead Diameters, electrospun under 15 kV and 1.3 mm³/s.

Solution Type(BR/UHMWPE)	Distance (mm)	Nominal Fiber Diameter (μm)	Nominal Bead Diameter (μm)
15/20	80	2.20 ± 0.50	60 ± 40
15/20	100	3.10 ± 1.00	40 ± 30
15/20	150	5.10 ± 2.00	25 ± 15
18/20	80	2.80 ± 1.20	80 ± 60
18/20	100	2.40 ± 0.90	45 ± 25
18/20	150	5.60 ± 3.50	20 ± 10

4.3. Feed Rate

The final process parameter examined is the feed rate, and was accomplished by fixing the subsidiary conditions at 15 kV and 100 mm. The reason why these values were picked is due to the smooth formation of the cone and the regular flow geometry that occurs between the nozzle and the collector plate. On the other hand, the feed rate values must be selected carefully so that no excessive solvent drops flow down to the ground from the tip of the nozzle. Otherwise, the flow geometry is deteriorated and the viscous forces start approaching the electrical forces, endangering the spinning operation. Another danger that must be avoided is the possibility of the electrical arc formation between the nozzle and the collector.

Taking these measures into account, the feed rate values were altered in three steps, 0.83 mm³/s, 1.3 mm³/s and 1.65 mm³/s for two different polymer blends, 15/20 (BR/UHMWPE) and 18/20 (BR/UHMWPE) due to the decent flowing geometry between the nozzle and the collector. The SEM images of the resultant fibers are provided in Figures 4.13 to 4.18, and are summarized in Table 4.5.

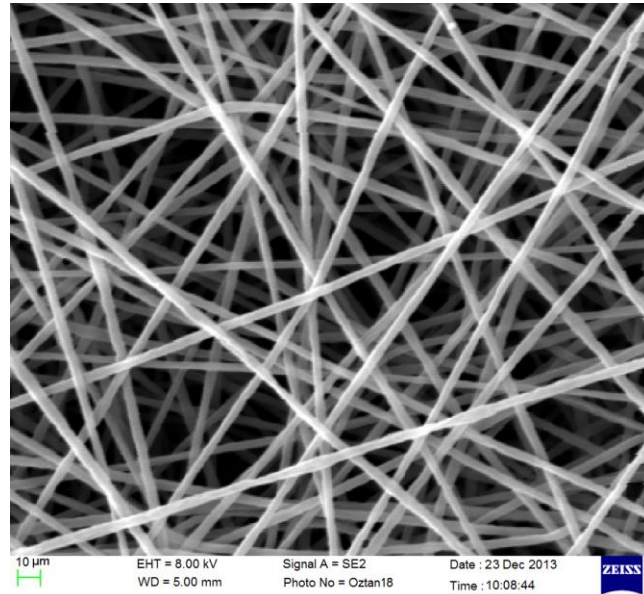


Figure 4.13. SEM image of 18/20 wt% (BR/UHMWPE) electrospun with 0,83 mm³/s.

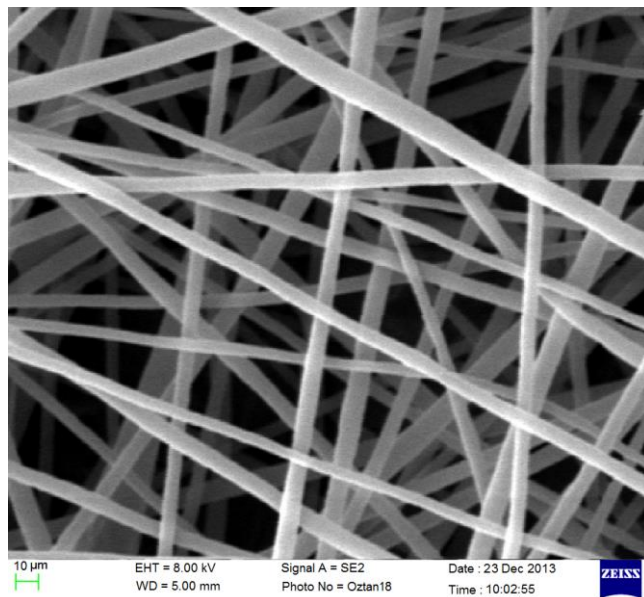


Figure 4.14. SEM image of 18/20 wt% (BR/UHMWPE) electrospun with 1,30 mm³/s.

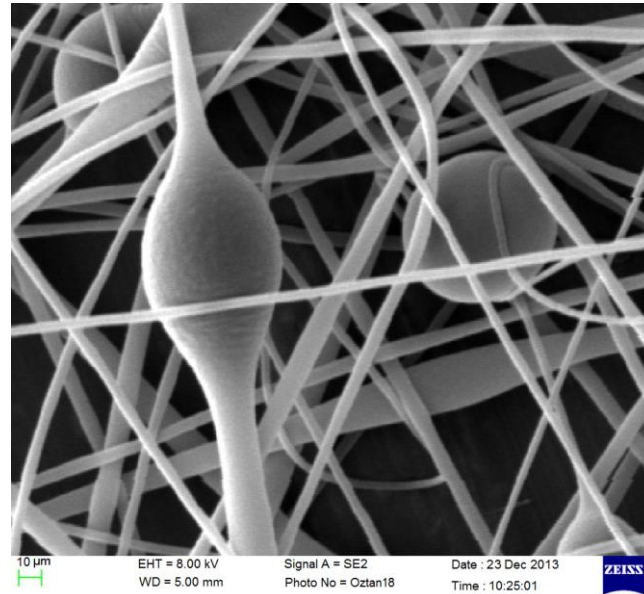


Figure 4.15. SEM images of 18/20 wt% (BR/UHMWPE) electrospun with 1,65 mm³/s.

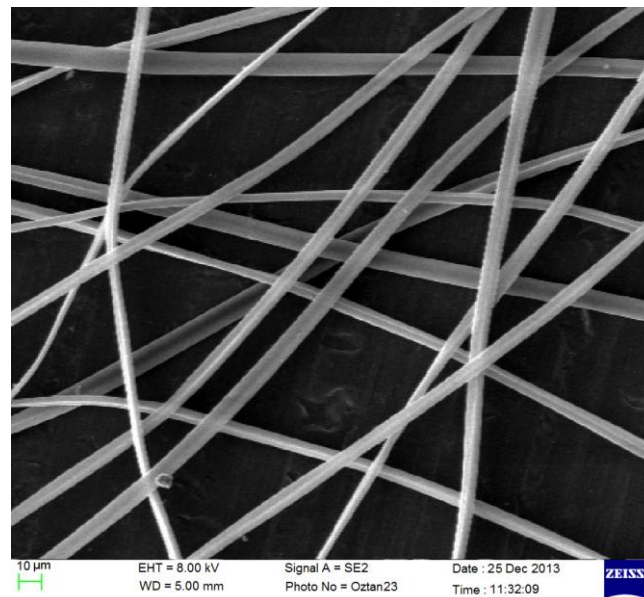


Figure 4.16. SEM images of 15/20 wt% (BR/UHMWPE) electrospun with 0,83 mm³/s.

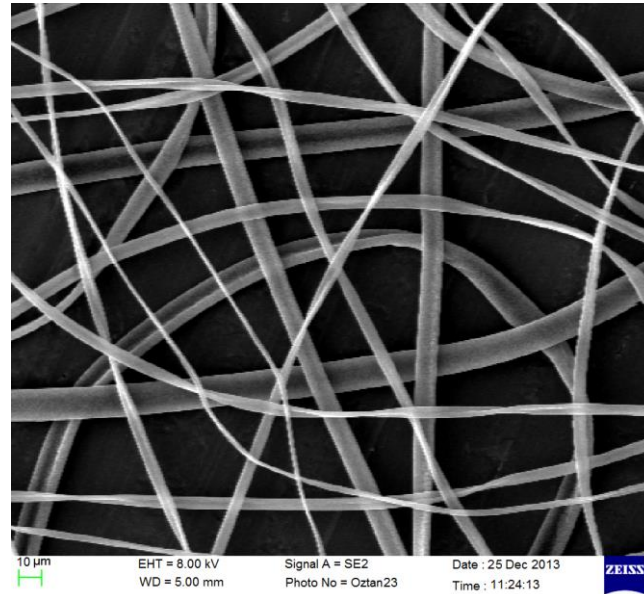


Figure 4.17. SEM images of 15/20 wt% (BR/UHMWPE) electrospun with $1,30 \text{ mm}^3/\text{s}$.

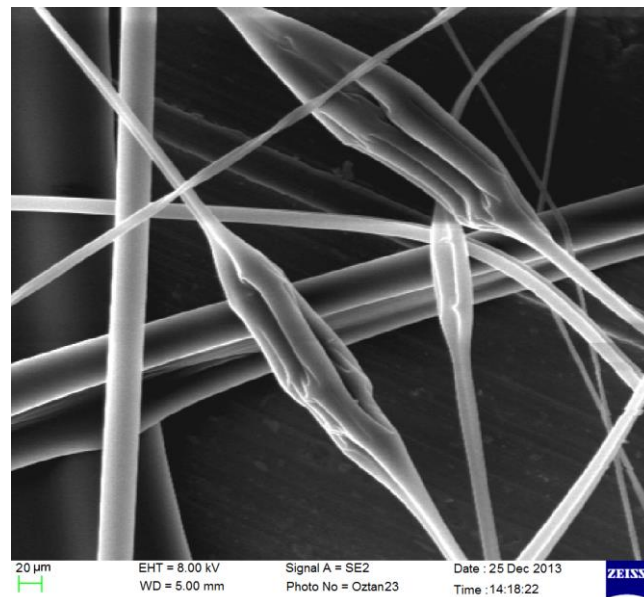


Figure 4.18. SEM images of 15/20 wt% (BR/UHMWPE) electrospun with $1,65 \text{ mm}^3/\text{s}$.

Table 4.5. Correlation of concentration, feed rate and fiber diameters, electrospun under 15 kV and 100 mm.

Solution Type wt% (BR/UHMWPE)	Feed Rate (mm ³ /s)	Nominal Fiber Diameter (μm)
15/20	0.83	8.50 ± 3.70
15/20	1.30	7.60 ± 3.40
15/20	1.65	16.10 ± 7.20
18/20	0.83	5.00 ± 0.50
18/20	1.30	6.20 ± 2.20
18/20	1.65	8.10 ± 5.70

5. CONCLUSIONS

Ultra High Molecular Weight Polyethylene / Butyl Rubber fibers that were produced in the experiments yielded with diameters between 2.40 and 16.10 μm . In compliance with as it was stated in the introduction chapter, the fiber diameters exceeded 100 nm, which is the limit condition to be counted as nanofiber so the resultant fibers cannot be counted as nanofibers. Instead, they are taken as microfibers.

Because the majority of the materials were like the ones in Göktaş's studies, apart from the usage of UHMWPE in this study, the evaluation can be performed as a comparison among the two studies. Due to the great affinity of the densities of UHMWPE and Polystyrene, which Göktaş used in his experiments, the resultant fiber morphologies seen under SEM were close, too.

On the other hand, the results of the other significant study on electrospinning of UHMWPE fibers, which was performed by Rein and his team, showed great differences from this study. The main reason why such a difference occurred is that Rein utilized two different and very volatile (and surface tension reducing) solvents to regulate the viscosity (thus the surface tension) in the solution, which are Cyclohexanone and P-Xylene. Utilization of these solvents allowed Rein's team to keep the UHMWPE weight percentages in much less ratios than the ones in this study. Another reason why such huge difference in weight percentage values is the alteration of temperature in Reins's study, where the UHMWPE mixtures were heated up to 130 °C, causing a significant reduce in viscosity, whereas this study utilized solvents in ambient temperature. At all, the SEM images taken in Rein's studies stayed well above the nano limit, 100 nm.

The effects of the three major process parameters on the morphology of the resultant fibers were also studied. For each parameter, the change of fiber morphology is provided in the figures 5.1 to 5.5.

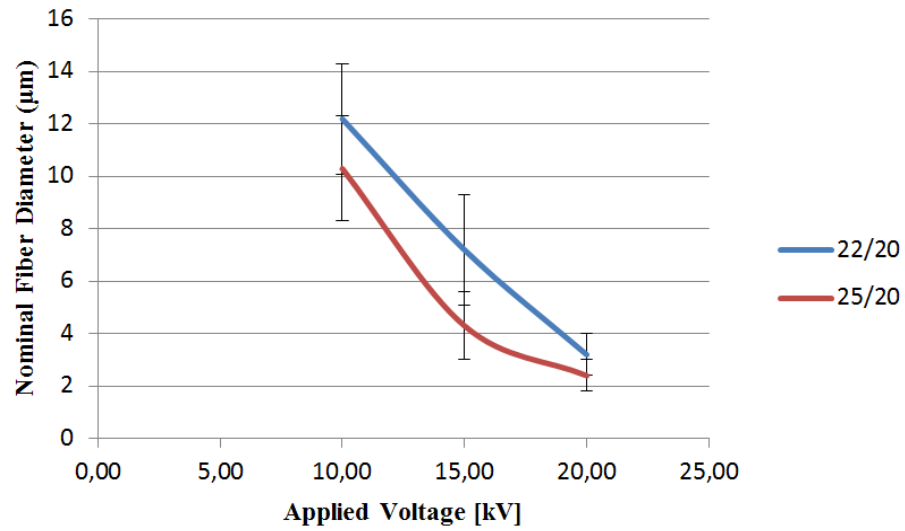


Figure 5.1. Change of nominal fiber diameter with applied voltage.

According to the figure, nominal fiber diameter values decreased, meaning the fibers got finer, as applied voltage was increased. Secondly, as the concentration was increased, the resultant fibers got coarser. The results totally comply with the theory.

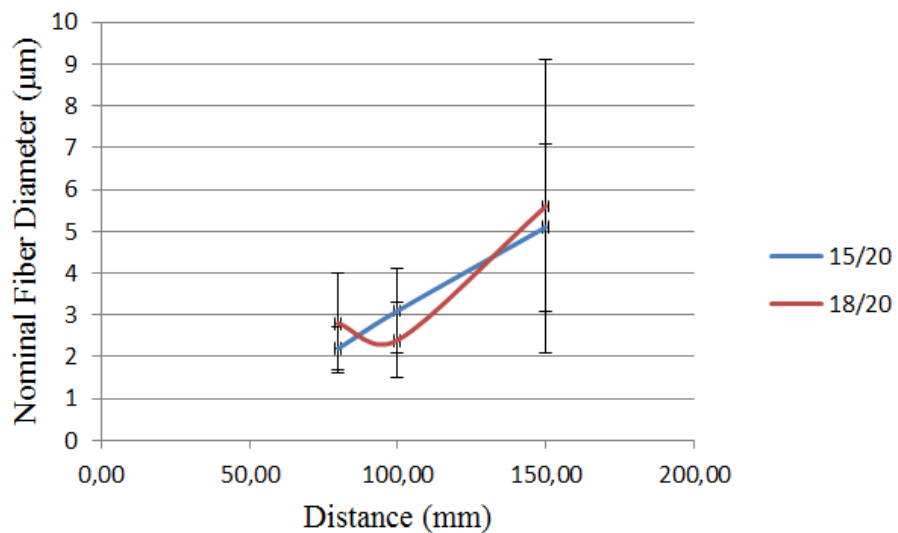


Figure 5.2. Change of nominal fiber diameter with distance.

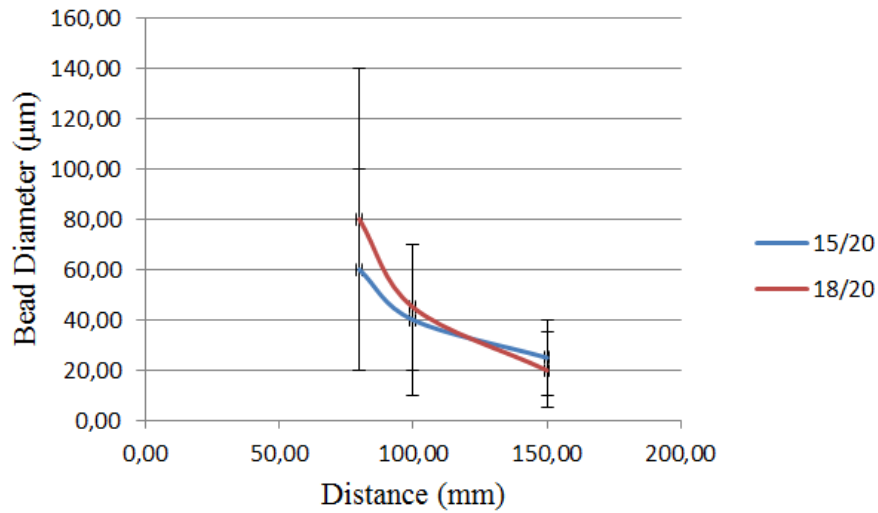


Figure 5.3. Change of nominal bead diameter with distance.

Taking the results for both solutions into account, the fibers got coarser and the beads got finer as the distance was increased. The results partially comply with the theory for finer fibers were expected. The main reason why such a congested result was obtained is the proximity of viscous forces to electrical forces required for formation of the Taylor cone. Thanks to this proximity, the fibers could not get finer in diameter but yielded with finer beads that have a less threshold value for formation. On the other hand, due to the activation of bead formation mechanism because of the higher surface tension forces, beads formed and complied with the theory. The secondary reason why this occurred is the conductivity of the solution. It might have been increased by either adding more NaCl, or more qualitative salts, like LiCl. As a result, the fibers could have been exposed to more electrical forces, thus overcome the viscous forces more easily.

Göktaş's studies yielded with finer fibers, which had a minimum fiber diameter of about 0,76 µm. Apart from the results in this thesis; he did not observe significant diameter changes when the distance was altered. Utilization of CuCl₂ as surfactant also caused minor differences in Göktaş's thesis. Since no other surfactants were added in this study, alternative surfactant mixtures still remain an undiscovered issue for Butyl Rubber and UHMWPE.

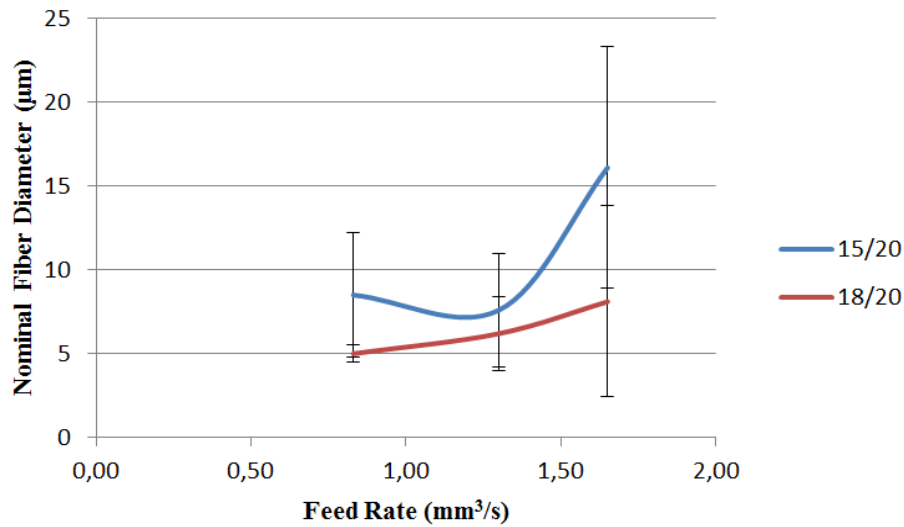


Figure 5.4. Change of nominal fiber diameter with feed rate.

As for the results of the feed rate parameter, 18/20 solutions exhibited an expected behavior; meaning as the rate was increased, the fibers got coarser for they were travelled from the nozzle to the screen in a less time, which caused them to be exposed to electrical forces for shorter times, so the results are expected. Meanwhile, the 15/20 solution exhibited a partially expected behavior, meaning it yielded with finer fibers for 10%, as the rate was increased thus belying the theory at first sight, but then gradually got coarser for twice and complied with the theory. With the informational background introduced in this thesis, this result cannot be explained, giving the weak link of the study.

The experiments in this thesis were performed only with single pump on which two parallel syringes were mounted, meaning both polymers were ejaculated with the same feed rate. Connecting one more pump with a distinct rate could give more theory – complying results, due to the different Taylor Cone thresholds required for different polymers, thanks to their distinct viscosities. Such a modification in the experimental setup is sure to improve the spinning performance, giving more decent spinning geometries.

REFERENCES

1. Formhals, A., *1975504 U.S. Patent*, Editor. 1934.
2. Kurtz, S. M., *UHMWPE Biomaterials Handbook, Second Edition: Ultra High Molecular Weight Polyethylene of Total Joint Replacement and Medical Devices*, 2009.
3. Polymer Fundamentals: Fiber Applications, <http://www.fibersource.com/f-tutor/poly.htm>, 2012, [Accessed December 2013].
4. Raghavendra R., Dahiya, M., Kamath, G., “Nonwoven Nanofibers”, *International Fiber Journal*, 2005.
5. Bajakova, J., J. Chaloupek, *The Production of Individual Nanofibers by Experimental Method*, 2011.
6. Mittal, V., *In-situ Synthesis of Polymer Nanocomposites*, Wiley-Verlag, München, 2011.
7. Liu, X., Y. Wang, X. Song, *Role of Thermal Process on Self-assembled Structures of 4'-([2,2':6',2''-Terpyridin]-4'-Yl)-[1,1'-Biphenyl]-4-Carboxylic Acid on Au(III)*, 2013.
8. Wood, A., *Polymer Phase Separation Lecture Notes*, Concordia Press, Saskatchewan, 2011.
9. Boudriot, U., *Electrospinning Approaches to Scaffold Engineering - A Brief Overview on Artificial Organs*, New Delhi Press, 2006.

10. Saito, N., N. Murakami, J. Takahashi, H. Horiuchi, *Synthetic Biodegradable Polymers as Drug Delivery Systems for Bone Morphogenetic Proteins with Advanced Drug Delivery Reviews*, pp. 11-12, 2005.
11. Willerth, S., *Approaches to Neural Tissue Engineering Using Scaffolds for Drug Delivery and Advanced Drug Delivery Reviews*, pp. 325-326, 2007.
12. Safi, S., "Study of Electrospinning of Sodium Alginate, Blended Solutions of Sodium Alginate/Poly (Vinyl Alcohol) and Sodium Alginate/Poly (Ethylene Oxide)", *Journal of Applied Polymer Science*, pp. 3245-3256, 2007.
13. Sharma, P., "Structure and Assembly of PEO-PPO-PEO Co-Polymers of Mammalian Cell-Culture Media", *Journal of Biomaterials Science, Polymer Edition*, Vol. 16, pp. 1139-1151, 2005.
14. Doshi, J., D. Reneker, "Electrospinning Process and Applications of Electrospun Fibers", *Journal of Electrostatics*, Vol. 35, pp. 2-3, 1995.
15. Taylor, G., "Electrically Driven Jets", *Proceedings of the Royal Society of London, Mathematical and Physical Sciences*, Vol. 313, pp. 453-475, 1969.
16. Tripatanasuwan, S., Z. Zhong, D. Reneker, *Effect of Evaporation and Solidification of the Charged Jet of Electrospinning of Poly (Ethylene Oxide) Aqueous Solution*, pp. 42-46, 2007.
17. Fong, H., I. Chun, H. Reneker, "Beaded Nanofibers Formed during Electrospinning", *Polymer*, Vol. 40, pp. 422-428, 1999.
18. Deitzel, J., "The Effect of Processing Variables on the Morphology of Electrospun Nanofibers and Textile", *Polymer*, Vol. 42, pp. 261-272, 2001.

19. Yarin, L., S. Koombhongse, D. Reneker, "Bending Instability of Electrospinning of Nanofibers", *Journal of Applied Physics*, Vol. 81, p. 3018, 2001.
20. Reneker, D., A. Yarin, H. Fong, S. Koombhongse, "Bending Instability of Electrically Charged Liquid Jets of Polymer Solutions of Electrospinning", *Journal of Applied Physics*, Vol. 87, pp. 4531-4547, 2000.
21. Hohman, M., M., Shin, G. Rutledge, M. Brenner, "Electrospinning and Electrically Forced Jets, Stability Theory", *Physics of Fluids*, Vol. 13, pp. 2201-2202, 2001.
22. Hohman, M., M., Shin, G. Rutledge, M. Brenner, "Electrospinning and Electrically Forced Jets, Applications", *Physics of Fluids*, vol 13, pp. 2221-2236, 2001.
23. Huang, Z., M. Zhang, Y. Kotaki, S. Ramakrishna, "A Review on Polymer Nanofibers by Electrospinning and Applications of Nanocomposites", *Composites Science and Technology*, Vol. 63, pp. 2223-2225, 2003.
24. Buer, A., S. Ugbolue, S. Warner, "Electrospinning and Properties of Some Nanofibers", *Textile Research Journal*, Vol. 71, pp. 323-328, 2001.
25. Scardino, L., R. Balonis, *US Patent 6106913*, 2000.
26. Baumgarten, P., *Colloid Interface Technology*, pp. 71-79, McGraw Hill, New York, 1971.
27. Larrondo, L., R. Manley, "Polymer Physics", *Journal of Polymer Science*, Vol.19, pp. 909-911, 1981.
28. Larrondo, L., R. Manley, "Polymer Physics", *Journal of Polymer Science*, Vol.19, pp. 921-932, 1981.

29. Larrondo, L., R. Manley, "Polymer Physics", *Journal of Polymer Science*, Vol.19, pp. 933-940, 1981.
30. Gupta, P., *Processing-Structure-Property Studies of: I) Submicron Polymeric Fibers Produced by Electrospinning and II) Films of Linear Low Density Polyethylenes as Influenced by The Short Chain Branch Length of Copolymers of Ethylene/1-Butene, Ethylene/1-Hexene & Ethylene/1-Octene Synthesized by a Single Site Metallocene Catalyst*, Virginia Tech. Press, Virginia, 2004.
31. Koombhongse, S., W. Liu, D. Reneker, "Flat Ribbons and Other Shapes by Electrospinning", *Journal of Polymer Science and Polymer Physics*, Vol. 39, pp. 2598-2606, 2001.
32. Electrospinning, <http://www.che.vt.edu/Faculty/electrospinning/electrospinning.html>, 2012, [Accessed December 2013].
33. Reneker, D., H. Chun, "Nanometre Diameter Fibres of Polymer, Produced by Electrospinning", *Nanotechnology*, Vol. 7, pp. 216-223, 1996.
34. McTaylor, G., "Electrically Driven Jets", *Proceedings of Royal Society of London*, Vol. 313, pp. 453-475, 1969.
35. Subbiah, T., G. Bhat, R. Tock, W. Parameswaran, S. Ramkumar, "Electrospinning of Nanofibers", *Journal of Applied Polymer Sciences*, Vol. 96, pp. 557-569, 2005.
36. Reneker, D., A. Yarin, H. Fong, S. Koombhongse, "Bending Instability of Electrically Charged Liquid Jets of Polymer Solutions of Electrospinning", *Journal of Applied Physics*, Vol. 87, pp. 4531-4547, 2009.
37. Shin, Y., M. Hohman, M. Brenner, G. Rutledge, "Electrospinning: A Whipping Fluid Jet Generates Submicron Polymer Fibers", *Applied Physics Letters*, Vol. 78, pp.

- 1149-1151, 2001.
38. Doshi, J., D. Reneker, "Electrospinning and Applications of Electrospun Fibers", *Industrial Application Society Annual Meeting Journal*, Vol. 3, pp. 1698-1703, 1993.
 39. Frenot, A., I. Chronakis, "Polymer Nanofibers Assembled by Electrospinning", *Current Opinion in Colloid and Interference Science*, Vol. 8, pp. 64-75, 2003.
 40. Rutledge, C., M. Shin, S. Warner, A. Buer, M. Grimler, M. Ugbolue, "Investigation on the formation and Properties of the Electrospun Fibers", *National Textile Center Annual Report*, pp. 35-36, 2000.
 41. Wannatong, L., A. Sirivat, P. Supaphol, "Effects of Solvents on Electrospun Polymer Fibers: Preliminary Study on UHMWPE", *Polymer International*, Vol. 53, pp. 1851-1859, 2004.
 42. Huang, Z., Y. Zhang, M. Kotaki, S. Ramakrishna, "A Review on Polymer Nanofibers by Electrospinning and Their Applications of Nanocomposites", *Composite Science and Technology*, Vol. 63, pp. 2223-2253, 2003.
 43. Ramakrishna, S., K. Fujihara, W. Teo, T. Lim, Z. Ma, "An Introduction to Electrospinning and Nanofibers", *World Scientific Publishing*, Vol. 21, pp. 2211-2214, 2008.
 44. Jarusuwannapoom, T., W. Hangrojjanawiwat, S. Jitjaicham, L. Wannatong, M. Nithitanakul, C. Pattamaprom, P. Koombhongse, R. Rangkupan, P. Supaphol, "Effect of Solvents on Electrospinnability of UHMWPE Solutions and Morphological Appearance of Resulting Electrospun UHMWPE Fibers", *European Polymer Journal*, Vol. 41, pp. 409-421, 2005.
 45. Mituppatham, C., M. Nithitanakul, P. Supaphol, "Ultrafine Electrospun Polyamide-6

- Fibers: Effect of Solution Conditions on Morphology and Average Fiber Diameter”, *Macromolecule Chemistry Physics*, Vol. 205, pp. 2327-2338, 2004.
46. Choi, J., S. Lee, L. Jeong, S. Bae, B. Min, J. Youk, W. Park, “Effect of Organosoluble Salts on the Nanofibrous Structure of Electrospun Poly (3-Hydroxybutyrate-Co-3-Hydroxyvalerate)”, *International Journal of Biological Macromolecules*, Vol. 34, pp. 249-256, 2004.
 47. Son, W., J. Youk, T. Lee, W. Park, “The Effects of Solution Properties and Polyelectrolyte on Electrospinning of Ultrafine Poly (Ethylene Oxide) Fibers”, *Polymer*, Vol. 45, pp. 2959-2966, 2004.
 48. Lin, T., H. Wang, “The Charge Effect of Cationic Surfactants on the Elimination of Fiber Beads of the Electrospinning of UHMWPE”, *Nanotechnology*, Vol. 15, pp. 1375-1381, 2004.
 49. Fong, H., I. Chun, D. Reneker, “Beaded Nanofibers Formed during Electrospinning”, *Polymer*, Vol. 40, pp. 4585-4592, 1999.
 50. Yang, Q., Z. Li, Y. Hong, “Influence of Solvents on the formation of Ultrathin Uniform Poly (Vinyl Pyrrolidone) Nanofibers of Electrospinning”, *Journal of Polymer Science Part B : Polymer Physics*, Vol. 42, pp. 3721-3726, 2007.
 51. Zeng, J., X. Xu, X. Chen, Q. Liang, X. Bian, L. Yang, X. Jing, “Biodegradable Electrospun Fibers for Drug Delivery”, *Journal of Controlled Release*, Vol. 92, pp. 227-231, 2003.
 52. Drew, C., X. Wang, L. Samuelson, J. Kumar, “The Effect of Viscosity and Filler on Electrospun Fiber Morphology”, *Journal of Macromolecules Science*, Vol. 40, pp. 1415-1422, 2003.

53. Shenoy, S., D. Bates, H. Frisch, G. Wnek, "Role of Chain Entanglements on Fiber Formation during Electrospinning of Polymer Solutions: Good Solvents, Non-Specific Polymer-Polymer Interaction Limit", *Polymer*, Vol. 46, pp. 3372-3384, 2005.
54. Koski, A., Yim, K., Shivkumar, S., *Effect of Molecular Weight on Fibrous PVA Produced by Electrospinning*, *Mater. Let.* 2004, 58, 493-497.
55. Megelski, S., J. Stephens, D. Chase, J. Robalt, "Micro and Nanostructured Surface Morphology on Electrospun Polymer Fibers", *Macromolecules*, Vol. 35, pp. 8456-8466, 2002.
56. Zheng, J., A. He, J. Li, J. Xu, C. Han, "Studies on the Controlled Morphology and Wettability of UHMWPE Surfaces by Electrospinning or Electrospraying", *Polymer*, Vol. 47, pp. 7095-7102, 2006.
57. Casper, C., J. Stephens, N. Tassi, D. Chase, J. Rabolt, "Controlling Surface Morphology of Electrospun UHMWPE Fibers: Effect of Humidity and Molecular Weight in the Electrospinning Process", *Macromolecules*, Vol. 37, pp. 573-578, 2004.
58. Matthews, J., A. Wnek, D. Simpson, G. Bowlin, "Electrospinning of Collagen Nanofibers", *Biomacromolecules*, Vol. 3, pp. 232-238, 2002.
59. Lee, K., H. Kim, H. Bang, Y. Jung, S. Lee, "The Change of Bead Morphology Formed on Electrospun UHMWPE Fibers", *Polymer*, Vol. 44, pp. 4028-4034, 2003.
60. Wang, C., H. Hsu, J. Lin, "Scaling Laws in Electrospinning of UHMWPE Solutions", *Macromolecules*, Vol. 39, pp. 7662-7672, 2006.
61. Baker, S., N. Atkin, P. Gunning, N. Granville, K. Wilson, D. Wilson, J. Southgate,

- “Characterisation of Electrospun UHMWPE Scaffolds for Three-Dimensional of Vitro Biological Studies”, *Biomaterials*, Vol. 27, pp. 3136-3146, 2006.
62. Zeng, J., X. Chen, X. Xu, Q. Liang, X. Bian, L. Yang, L. X. Jing, “Ultrafine Fibers Electrospun from Biodegradable Polymers”, *Journal of Applied Polymer Science*, Vol. 89, pp. 1085-1092, 2003.
63. Casper, C., J. Stephens, N. Tassi, D. Chase, J. Rabolt, “Controlling Surface Morphology of Electrospun UHMWPE Fibers: Effect of Humidity and Molecular Weight in the Electrospinning Process”, *Macromolecules*, 2004.
64. Gupta, P., C. Elkins, T. Long, G. Wilkes, “Electrospinning of Linear Homopolymers of Poly (Methyl Methacrylate), Exploring Relationships between Fiber Formation, Viscosity, Molecular Weight and Concentration of a Good Solvent”, *Polymer*, Vol. 46, pp. 4799-4810, 2005.
65. Lee, K., H. Kim, M. Khil, Y. Ra, D. Lee, “Characterization of Nanostructured Poly (C-Caprolactone) Nonwoven Mats Via Electrospinning”, *Polymer*, Vol. 44, pp. 1287-1294, 2003.
66. Deitzel, J., T. Beck, J. Kleinmeyer, J. Rehrmann, D. Tevault, D. Reneker, I. Sendjarevic, A. McHugh, “Generation of Polymer Nanofibers through Electrospinning”, *Polymer*, Vol. 33, pp. 1171-1176, 2002.
67. Greiner, A., J. Wendorff, "Electrospinning: A Fascinating Method for the Preparation of Ultrathin Fibers", *Angewandte Chemistry International Edition*, Vol. 46, pp. 5670-5703, 2007.
68. Sun, D., C. Chang, S. Li, L. Lin, “Near Field Electrospinning”, *Nanoletters*, Vol. 6, pp. 839-842, 2006.

69. Courtney D., *Ionic Liquid Ion Source Emitter Arrays Fabricated on Bulk Porous Substrates for Spacecraft Propulsion*, Ph.D. thesis, Massachusetts Institute of Technology, 2011.
70. Shibata, N., S. Kurtz, N. Tomita, "Recent Advances of Mechanical Performance and Oxidation Stability in Ultra High Molecular Weight Polyethylene for Total Joint Replacement: Highly Crosslinked and Tocopherol Doped", *Journal of Biomechanical Science and Engineering*, Vol. 10, pp. 107-123, 2006.
71. Hanna, R., *Handbook of Plastic Materials and Technology*, J. Wiley and Sons, New York, 1990.
72. Edidin, A., S. Kurtz, "The Influence of Mechanical Behavior on the Wear of Four Clinically Relevant Polymeric Biomaterials of A Hip Simulator", *Journal of Arthroplasty*, Vol. 15, pp. 321-331, 2000.
73. Prevorsek, D., "Trends in Polymers", *Polymer Science*, pp. 4-11, 1995.
74. Andreopoulos, A., "Polymer Advances in Technology", *Economy*, Vol. 5, pp. 349-357, 1994.
75. Smith, P., J. Lemstra, "Processing of Polymers Using Reactive Solvents", *Material Science*, Vol. 15, pp. 505-514, 1980.
76. Barham, P., A. Keller, "Handbook of Fiber Science and Technology", *Material Science*, Vol. 20, pp. 2281-2302, 1985.
77. Kavesh, S., D. Prevorsek, "Producing Modified High Performance Polyolefin Fiber", *International Journal of Polymer Materials*, Vol. 30, pp. 55-56, 1995.
78. Larrondo, L., R. Manley, "A View on Polymers", *Journal of Polymer Science*, Vol.

- 19, pp. 1294-1301, 2003.
79. Rein, D., L. Shavit, L. Khalfin, “Electrospinning of Ultra High Molecular Weight Polyethylene”, *Journal of Polymer Science Part B: Polymer Physics*, Vol. 19, pp. 909-920, 1981.
 80. Butyl Rubber - Polyisobutylene, <http://www.azom.com/article.aspx?ArticleID=1549>, Retrieved from Azom, 2013, [Accessed December 2013].
 81. Gökteş A., *Electrospinning of Polystyrene/Butyl Rubber Blends: A Parametric Study*, M.S. Thesis, Middle East Technical University, 2008.
 82. Viriyabanthorn, N., J. Mead, R. Stacer, G. Sung, “Effect of Carbon Black Loading on Electrospun Butyl Rubber Nonwoven Mats”, *Polymer Preprints*, Vol. 44, pp. 136-137, 2003.
 83. Threepopnatkul, P., D. Murphy, J. Mead, “Effects of Carbon Black Type on Breathable Butyl Rubber Membranes”, *25th American Chemists Society Handbook*, Orlando, Florida, 2006.